Development 140, 2776-2786 (2013) doi:10.1242/dev.091876

The zebrafish common cardinal veins develop by a novel mechanism: lumen ensheathment

Christian S. M. Helker[1], Annika Schuermann[1], Terhi Karpanen[2], Dagmar Zeuschner[3], Heinz-Georg Belting[4], Markus Affolter[4], Stefan Schulte-Merker[2,5] and Wiebke Herzog[1,3,*]

SUMMARY

The formation and lumenization of blood vessels has been studied in some detail, but there is little understanding of the morphogenetic mechanisms by which endothelial cells (ECs) forming large caliber vessels aggregate, align themselves and finally form a lumen that can support blood flow. Here, we focus on the development of the zebrafish common cardinal veins (CCVs), which collect all the blood from the embryo and transport it back to the heart. We show that the angioblasts that eventually form the definitive CCVs become specified as a separate population distinct from the angioblasts that form the lateral dorsal aortae. The subsequent development of the CCVs represents a novel mechanism of vessel formation, during which the ECs delaminate and align along the inner surface of an existing luminal space. Thereby, the CCVs are initially established as open-ended endothelial tubes, which extend as single EC sheets along the flow routes of the circulating blood and eventually enclose the entire lumen in a process that we term 'lumen ensheathment'. Furthermore, we found that the initial delamination of the ECs as well as the directional migration within the EC sheet depend on Cadherin 5 function. By contrast, EC proliferation within the growing CCV is controlled by Vascular endothelial growth factor C, which is provided by circulating erythrocytes. Our findings not only identify a novel mechanism of vascular lumen formation, but also suggest a new form of developmental crosstalk between hematopoietic and endothelial cell lineages.

KEY WORDS: Cadherin 5, Vegfc, Angioblast specification, Collective migration, Common cardinal vein, Lumen formation

INTRODUCTION

To supply the body with oxygen and nutrients, a complex vascular network of arteries, veins and capillaries is formed, with individual blood vessels being specifically adapted to their respective functions. Differences between these individual blood vessel types are reflected in their specific cellular architecture and physiological function, as well as in their differential development and by marked differences in gene expression profiles (reviewed by Dyer and Patterson, 2010; Atkins et al., 2011).

Formation of the zebrafish vasculature (reviewed by Ellertsdóttir et al., 2010) commences at 12 hours post-fertilization with the specification of angioblasts within the lateral plate mesoderm. These migrate to the embryonic midline, where they coalesce into a vascular cord (Jin et al., 2005), giving rise to the dorsal aorta (DA) and the posterior cardinal vein (PCV) (Torres-Vázquez et al., 2003). Recently, it was proposed that in the caudal region of the zebrafish embryo individual venous-fated endothelial cells (ECs) leave the initial vascular cord and migrate ventrally to form the vein, while the remaining ECs differentiate into the DA (Herbert et al., 2009). However, a detailed analysis of cardinal vein formation in zebrafish or mice has yet to be carried out.

To form definitive lumenized vessels, 'budding', 'cord hollowing', 'cell hollowing' and 'cell membrane invagination' have all been described as mechanisms of vascular lumen formation (Baer et al., 2009; Iruela-Arispe and Davis, 2009; Ellertsdóttir et al., 2010; Herwig et al., 2011). During DA formation in both zebrafish and mice, ECs form a lumen by a process called cord hollowing, which is a mechanism by which a set of compact cells undergoes shape changes to create a central lumen (Jin et al., 2005; Strilić et al., 2009). It is generally believed that the cardinal veins form their lumen by the same mechanism.

Further angiogenic growth depends on EC migration and proliferation. Proteins of the vascular endothelial growth factor (Vegf) family, especially Vegfa, have been implicated in regulating different steps of EC development, including specification, migration and proliferation (reviewed by Veikkola and Alitalo, 1999; Carmeliet, 2000). Although Vegfa is important for artery formation and specification, it appears not to be involved in venous development (Lawson and Weinstein, 2002b; Wiley et al., 2011). By contrast, Vegfc signaling, mainly via Vegf receptor 3 (Flt4) (Joukov et al., 1996; Lee et al., 1996; Hogan et al., 2009b), plays a major role in regulating the development of venous sprouts from the PCV and of the lymphatic vasculature (Karkkainen et al., 2004; Küchler et al., 2006; Yaniv et al., 2006).

In the present study we have examined the development of the common cardinal veins (CCVs). The CCVs are located in the anterior trunk of the embryo, where they collect all the venous blood and transport it to the heart. Whereas in the posterior region of the zebrafish the DA and the PCV are established as single tubes in the midline below the notochord, in the anterior part of the embryo these vessels split into two arteries [the lateral dorsal aortae (LDA)] and two cardinal veins, located on both sides of the midline (Fig. 1A). Emerging from these bilateral cardinal veins, the CCVs grow around either side of the yolk cell and converge cranioventrally at the sinus venosus of the heart, where they connect with the endocardial ECs (Isogai et al., 2001).

We have analyzed the development of the CCVs by *in vivo* time-lapse studies and cell tracing, as well as detailed gene expression

[1]University of Muenster, 48149 Muenster, Germany. [2]Hubrecht Institute-KNAW and UMC, 3584 CT Utrecht, The Netherlands. [3]Max Planck Institute for Molecular Biomedicine, 48149 Muenster, Germany. [4]Biozentrum der Universität Basel, CH-4056 Basel, Switzerland. [5]EZO, Wageningen University, NL-6700 AH Wageningen, The Netherlands.

*Author for correspondence (wiebke.herzog@mpi-muenster.mpg.de)

Accepted 24 April 2013

analysis and loss-of-function studies. We found that the development of the CCVs represents a completely novel mechanism of vessel formation, during which a distinct angioblast population forms the CCVs by aligning along the inner surface of an existing luminal space. Subsequently, the open CCV tubes extend by Cadherin 5-dependent EC migration and eventually enclose the entire lumen. Furthermore, we show for the first time that EC proliferation is controlled by Vegfc, which is provided by circulating blood cells.

MATERIALS AND METHODS

Zebrafish husbandry and strains

Zebrafish (*Danio rerio*) were maintained in a recirculating aquaculture system under standard laboratory conditions (Westerfield, 1993). All zebrafish experiments comply with the institutional and national animal welfare laws, guidelines and policies. Embryos were staged by hours post-fertilization (hpf) at 28.5°C (Kimmel et al., 1995).

The previously described zebrafish lines were *Tg(kdrl:EGFP)^{s843}* (Jin et al., 2005), *Tg(fli1a:EGFP)^{y1}* (Lawson and Weinstein, 2002a), *Tg(gata1:dsRed)^{sd2}* (Traver et al., 2003), *Tg(kdrl:HsHRAS-mCherry)^{s896}* (Chi et al., 2008), *Tg(fli1ep:GAL4FF)^{ubs4}* (Herwig et al., 2011), *Tg(UAS:KAEDE)^{rk8}* (Hatta et al., 2006), *Tg(etsrp:EGFP)^{ci1}* (Proulx et al., 2010) and *Tg(krt4:EGFP-caax)^{e112}* (Krens et al., 2011). *cdh5^{ubs8}* will be described in detail elsewhere (H.-G.B. and M.A., unpublished). The *vegfc^{hu6410}* allele encodes a stop codon at amino acid position 107 (L107Stop) and will be described in detail elsewhere (T.K. and S.S.-M., unpublished).

Generation of the *Tg(UAS:lifeact-GFP)^{mu271}* transgenic line

pT2UAS:lifeact-GFP was generated by cloning the coding sequence of lifeact-GFP (Riedl et al., 2008) into pT2UAS (Asakawa et al., 2008). pT2UAS:lifeact-GFP plasmid DNA (50 pg) was injected together with *tol2* transposase mRNA (250 pg). Three founder fish were identified and that with the brightest GFP expression was used in this study.

Microinjections

Microinjections of mRNA [synthesized using the Sp6 mMessage mMachine Kit (Ambion)] or morpholinos (MOs) were performed as previously described (Nasevicius and Ekker, 2000). *vegfc* mRNA (Hogan et al., 2009a), *H2B-cherry* mRNA (Santoro et al., 2007) or *sFLT4* mRNA (Mäkinen et al., 2001) were injected at 200 pg.

MOs targeting *tnnt2a* (Sehnert et al., 2002), *mitfa* (Robu et al., 2007), *sox32* (Chung and Stainier, 2008), *gata1* (Galloway et al., 2005) and *pu.1* (*spi1b* – Zebrafish Information Network) (Rhodes et al., 2005) have been described previously. mini-Ruby (tetramethylrhodamine, Invitrogen) was injected (0.1 ng) into the YSL as described previously (Sakaguchi et al., 2001).

Whole-mount *in situ* hybridization

Single *in situ* hybridizations were performed as described (Schulte-Merker, 2002; Thisse and Thisse, 2008); after staining, fixed embryos were further washed twice in methanol and cleared using a 2:1 mixture of benzylbenzoate:benzylalcohol. Double fluorescent *in situ* hybridizations were performed as described (Schoenebeck et al., 2007).

The following probes were synthesized as published: *flt4* (Lawson et al., 2001), *flt1* (Bussmann et al., 2007), *cdh5* (Larson et al., 2004) and *vegfc* (Hogan et al., 2009a).

etsrp (also known as *etv2*) was amplified from cDNA of 19-somite stage embryos using the following primers (5′-3′): *etsrp* forward, GAAAGGCCCAAGTCACAGAG; *etsrp* reverse, GAGTTCACTATCTGATGTCAAACCA. The T7 promoter was added to the 5′-end of the reverse primer in a second round of amplification: T7-*etsrp* reverse, GTAATACGACTCACTATAGGGAGTTCACTATCTGATGTCAAACCA.

In vivo time-lapse analysis, confocal microscopy and photoconversion

Embryos were manually dechorionated and mounted either in a 1% agarose embryo array (Megason, 2009) or in 0.3% agarose (with subsequent removal of agarose from the head/tail region). Medium and agarose were supplemented with a final concentration of 19.2 mg/l Tricaine and 30 mg/l phenylthiourea, respectively. For time-lapse imaging, embryos were kept in a 28.5°C heated chamber surrounding the microscope stage. All fluorescent images were acquired using an upright Leica Sp5 DM 6000, an inverse Leica Sp5 DM 6000, or a Zeiss LSM 780 confocal microscope. Confocal stacks and confocal movies were assembled using Imaris software (Bitplane). Color coding of images was performed using ImageJ (NIH).

For photoconversion, Kaede-positive double-transgenic embryos [*Tg(fli1ep:GAL4FF)^{ubs4};Tg(UAS:KAEDE)^{rk8}*] were photoconverted by scanning the anterior region of the embryo with a 405 nm diode laser in 3 μm steps using a Leica Sp5 DM 6000 inverse confocal microscope with a 10× objective. Photoconversion was monitored by the change in the Kaede emission wavelength from 518 nm (green channel) to 582 nm (red channel).

BrdU incorporation and immunohistochemistry

Embryos were incubated in 10 mM 5-bromo-2-deoxuridine (BrdU) for 30 minutes on ice and then grown at 28.5°C until the indicated time points and BrdU incorporation was detected as described (Herzog et al., 2009). The vasculature of the *Tg(kdrl:egfp)^{s843}* embryos was visualized using an anti-GFP Alexa 488 antibody (Invitrogen; 1:500).

The following antibodies were used: rabbit anti-zebrafish Cdh5 (Blum et al., 2008), mouse anti-human ZO-1 (TJP1) (Zymed), rabbit anti-zebrafish Podxl2 (Herwig et al., 2011) and Alexa 546 goat anti-rabbit, Alexa 568 goat anti-rabbit and Alexa 633 goat anti-mouse (Invitrogen). Immunohistochemistry was performed as described (Blum et al., 2008).

Quantifications

EC numbers were expressed relative to the average number counted in the CCVs of control embryos (set at 100%). The number of proliferating cells was quantified as the percentage of BrdU-positive among total ECs in the CCV. The length of the CCV was measured using the Measurement Point tool in Imaris. Using the manual Spot Track function in Imaris, the track length was calculated as the total length of displacements within the track, the migration speed was calculated as the track length divided by the time between the first and last object recorded, and the directionality was calculated as the ratio of the distance between the first and the last position and the track length.

Standard error of the mean (s.e.m.) and *P*-values using a two-tailed *t*-test were calculated using Microsoft Excel.

Fluorescence-activated cell sorting (FACS) of erythrocytes from zebrafish embryos

Tg(gata1:dsRed)^{sd2} zebrafish embryos were grown in the presence of 30 mg/l phenylthiourea. The yolk was removed by pipetting in PBS and centrifugation at 100 ***g*** for 3 minutes. A single-cell suspension was prepared by incubating with 0.25% trypsin-EDTA at 28.5°C for 30 minutes, with subsequent inactivation of trypsin by addition of 1% fetal bovine serum and filtration through a 70 μm cell strainer. dsRed^{+} and dsRed^{-} cells were sorted on a FACSAria II (Becton Dickinson) cell sorter and collected separately.

RNA isolation and semi-quantitative real-time PCR analysis

RNA was isolated from sorted cells using the PicoPure RNA isolation kit (Arcturus). RNA was reverse transcribed using Superscript II reverse transcriptase (Invitrogen). The cDNA was analyzed using the following primers (5′-3′, forward and reverse): β-*actin*, AATCCCAAAGCCAACAGAGA and CTTCTGCATACGGTCAGCAA; *gata1*, ATTATTCCACCAGCGTCCAG and CTGGCCGTTCATCTTATGGT; *vegfc*, CAGAAACAAGGTCGGAGGAG and TTCGGCATTCACACTGACAC.

Cryofixation and preparation of zebrafish embryos for electron microscopy

Anesthetized zebrafish embryos embedded in 1% agarose in gold-plated 200 μm deep specimen carriers were cryofixed by high-pressure freezing using a Leica HPM100. The samples were kept in liquid nitrogen until further processing.

For freeze substitution the samples were transferred to 1% OsO_4, 0.2% uranyl acetate, 5% water in acetone at −90°C. For 72 hours the sample was dehydrated and slowly fixed at low temperatures increasing to −30°C. The

samples were then transferred to 4°C for 1 hour and then further processed by embedding using Epon (Schieber et al., 2010). Within areas of interest, 60 nm ultrathin sections were cut on an ultramicrotome (Leica UC6). Sections were counterstained with uranyl acetate and lead, and analyzed using a transmission electron microscope (Tecnai-12-biotwin, FEI, Eindhoven, The Netherlands). Images were documented on image plates (Ditabis, Pforzheim, Germany).

RESULTS

Venous precursors of the cardinal veins and CCVs are specified as a separate population and at a different time point than arterial angioblasts

To analyze the development of the CCVs, we used *in vivo* confocal time-lapse imaging of the developing zebrafish trunk vasculature. We visualized individual angioblasts by transgenic GFP expression [*Tg(fli1a:EGFP)*^{y1}], which labels all ECs from the angioblast stage onwards.

We observed that the angioblasts in the trunk region of the zebrafish embryo are specified from posterior to anterior. Newly specified angioblasts are round in shape (arrowheads in Fig. 1B,D,F), before they change to an elongated form at the start of migration (arrows in Fig. 1B,E,F, Fig. 3A). At 14 hpf angioblasts are arranged in two parallel stripes within the lateral plate mesoderm (LPM). This first angioblast population migrates in towards the midline (arrows in Fig. 1B-D) and reaches its final position forming the LDA at 17 hpf (arrows in Fig. 1D, asterisks in 1E). At the same time, a second population of newly specified GFP-positive angioblasts with the characteristic round morphology (arrowheads in Fig. 1D-F) appears within the LPM. Some of these late-specified angioblasts start to migrate outwards to form the CCVs (arrows in Fig. 1F,G, Fig. 3A), whereas the other venous angioblasts form the bilateral cardinal veins (supplementary material Movie 1).

The time difference in the formation of the first and second angioblast populations is reflected by the temporal expression pattern of the early angioblast marker *ets related protein* (*etsrp*). Whereas angioblasts of the first population express *etsrp* at 12.5 hpf while they are located laterally within the LPM, this *etsrp* expression is lost after their migration to the midline (supplementary material Fig. S2). At 18 hpf the ECs forming the LDA are negative for *etsrp* (supplementary material Fig. S2D), but express other endothelial-specific genes such as *cadherin 5* (*vascular endothelial cadherin*, *cdh5*) (supplementary material Fig. S2E). At this time point, the later-specified angioblasts forming the anterior cardinal veins and the CCVs strongly express *etsrp* (supplementary material Fig. S2D), indicating that they are a distinct population of newly specified angioblasts. *etsrp* expression in the bilateral cardinal veins and CCVs is downregulated by 24 hpf (supplementary material Fig. S2F). In our confocal time-lapse observations of angioblast specification and movement, we do not see any mingling of these two angioblast populations (supplementary material Movie 1).

To analyze when the ECs of the forming CCVs and the bilateral cardinal veins acquire venous identity, we performed *in situ* hybridizations for arterial and venous-specific genes. Although it is known that arterial marker genes, such as *notch3* (Lawson et al., 2001) and *ephrin B2a* (Jin et al., 2005), only become expressed after angioblasts have migrated to their final position, we detected expression of *flt1* and *flt4* in all angioblasts of the forming trunk vessels (Fig. 2B,C,E,F,J-L, compare with *cdh5* in 2A,D,G). At later developmental stages (from 21 hpf onwards), *flt1* expression becomes restricted to the arteries (Fig. 2H) and *flt4* expression becomes restricted to the veins (Fig. 2I).

We therefore found no indication that arterial or venous identity is conveyed by gene expression at the individual angioblast level. Instead, the difference we observed is in the timing of angioblast

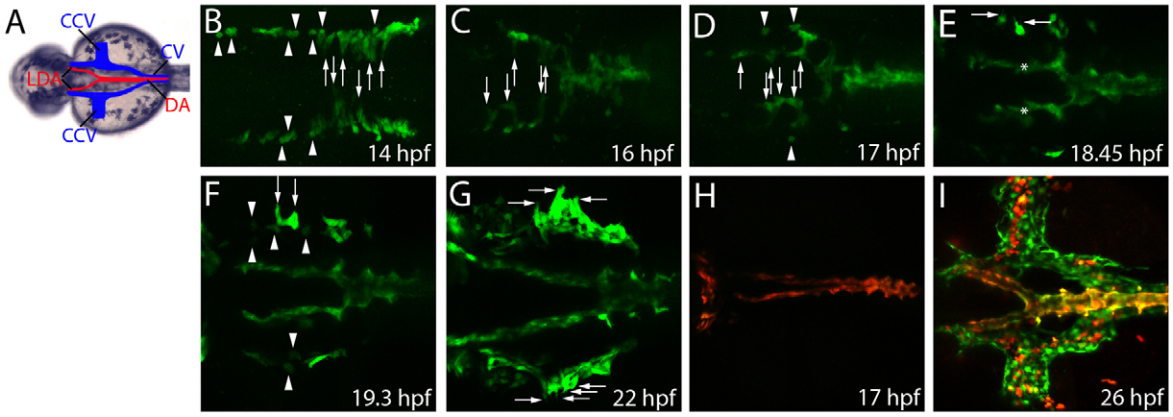

Fig. 1. Venous angioblasts become specified as a separate population and at a different time point than arterial angioblasts. (**A**) Trunk vasculature of a zebrafish embryo. Veins are pseudocolored blue and arteries red. (**B-G**) Confocal projections from a time-lapse movie of a *Tg(fli1a:EGFP)*^{y1} embryo. (B) At the time point of their specification, angioblasts appear to have a round morphology (arrowheads). The angioblast that will form the DA begin to migrate to the midline of the embryo (arrows). (C) While posterior angioblasts forming the DA arrive at the midline at 16 hpf, angioblasts forming the LDA have just started to migrate (arrows). (D) At 17 hpf, most of the LDA-forming angioblasts have arrived at their final position (arrows). At the same time, a second population of angioblasts of round morphology appears in the region where the bilateral cardinal veins will develop (arrowheads). (E) Angioblasts of this second population start to become elongated and form filopodia (arrows). Asterisks indicate the first population forming the LDA. (F) Additional GFP-positive angioblasts become specified (arrowheads). Some angioblasts of the second population have lost their round morphology and the first cells begin to migrate (arrows) to form the CCVs. (G) At 22 hpf, angioblasts with multiple filopodia migrate (arrows) to form the CCVs, whereas other angioblasts remain in a more central position to form the bilateral cardinal veins. (**H**,**I**) Merged confocal projections of the green and red channel showing Kaede protein expression in a *Tg(fli1ep:GAL4FF)*^{ubs}*;(UAS:KAEDE)*^{rk8} embryo. (H) Photoconversion of all endothelial cells (ECs) at 17 hpf, before the second population of angioblasts starts to express Kaede. Note that all ECs are photoconverted (red). (I) Arterial ECs in the LDA can be detected by both photoconverted (red) and new synthesized Kaede (green), whereas venous ECs in the bilateral cardinal veins and the CCVs only express newly synthesized Kaede (green). Note non-endothelial expression of Kaede by blood cells. All images represent dorsal views. Arrowheads, newly specified angioblasts; arrows, migrating angioblasts; DA, dorsal aorta; LDA, lateral dorsal aortae; CCV, common cardinal vein.

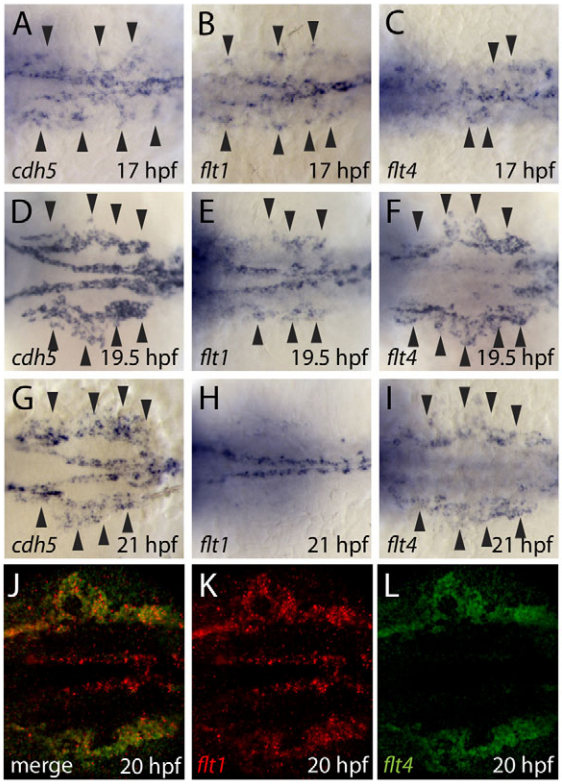

Fig. 2. All angioblasts show a common expression profile prior to arterial-venous differentiation. (**A-I**) Expression of *cdh5* (A,D,G), *flt1* (B,E,H) and *flt4* (C,F,I) detected by *in situ* hybridization (dorsal views). Arrowheads indicate the venous angioblasts. All angioblasts (A) and ECs of the arteries and veins (D,G) express *cdh5*. All angioblasts express *flt1* (B) and *flt4* (C), before *flt1* expression becomes downregulated in venous ECs (E,H) and *flt4* becomes downregulated in arterial ECs (F,I). (**J-L**) Double fluorescent *in situ* hybridization for *flt1* (red, J,K) and *flt4* (green, J,L) shows that individual angioblasts express *flt1* and *flt4* mRNA at the same time (at 20 hpf these are located in the veins, J).

specification. This difference in timing correlated with a difference in the migration of the angioblasts to their final anatomical location. Additionally, the differentiation into arterial or venous ECs only occurred after the cells had reached the position of the final vessels.

To directly test whether the time of angioblast specification determines their migration behavior, we used transgenic endothelial-specific expression of Kaede, a photoconvertible fluorophore (Ando et al., 2002; Hatta et al., 2006). Photoconversion of transgenic fish was performed at 17 hpf, before the second population of angioblasts turned Kaede positive (Fig. 1H). At 26 hpf all photoconverted red-fluorescing ECs were located in the LDA, whereas all cells of the CCVs expressed only newly synthesized, unconverted Kaede (visualized in green, Fig. 1I; supplementary material Fig. S1).

Hence, we provide evidence that the precursors of the CCV undergo a heterochronic development compared with the angioblasts that later form the LDA, as they become specified at different time points of development and subsequently adopt different migratory routes, guiding them to separate final positions.

Formation of the CCVs represents a new mode of blood vessel morphogenesis: lumen ensheathment

We continued to analyze the next steps in CCV development by confocal time-lapse microscopy. After the CCV angioblasts are specified within the second population, they migrate away from the midline between the yolk syncytial layer (YSL) and the epidermis and immediately start to align as a monolayer on top of the YSL (Fig. 3A-C′, Fig. 5A). Next, single angioblasts delaminate from the monolayer at the YSL side to the epidermal side (asterisks in Fig. 3E, Fig. 5B,C) to form a lumen before the onset of circulation (Fig. 3D-D″, Fig. 5D).

After delamination from the cellular sheet on top of the YSL (Fig. 3, Fig. 5B,C), the ECs forming the CCVs now align around a lumen and form open-ended tubes, which are sandwiched between the proximal YSL (Fig. 4B) and the distal epidermis (Fig. 4C). At the onset of blood flow, the CCVs are connected to the bilateral cardinal veins (midline side of the CCVs) and open towards the ventrolateral side, out of which the blood gushes into a space, which is free of ECs (Fig. 3D,D″, Fig. 4A,D; supplementary material Movie 2). The blood re-enters an EC-lined structure at the heart inflow tract (Fig. 4F,F′).

During further development, the ECs underneath the epidermis migrate collectively as a sheet (Fig. 3D′, Fig. 4C,J,K, Fig. 5E; supplementary material Movie 2) towards the endocardial ECs at the heart inflow tract (Fig. 4F,F′; supplementary material Movie 3). To analyze whether this rapid movement represents an active migration, we generated transgenic fish expressing lifeact-GFP (Riedl et al., 2008) under the control of a UAS promoter [*Tg(UAS:lifeact-GFP)*^{mu271}] and mated these with fish expressing Gal4 specifically in the vasculature [*Tg(fli1ep:GAL4FF)*^{ubs4}] (Herwig et al., 2011). Analysis of the double-transgenic offspring showed that the ECs forming the CCV indeed migrate actively, as indicated by the formation of actin-rich lamellipodia at the migration front (Fig. 4E,E′; supplementary material Movie 4).

To form the lumen, the ECs at the outer edges of the sheet start to fold inwards to engulf the blood stream (Fig. 4I,N, Fig. 5F). Consecutively, they fuse on the YSL side (Fig. 4L,L′; supplementary material Movie 5) in a dorsal to ventral sequence.

Interestingly, we could not detect apical EC polarization [analyzed by Podocalyxin-like 2 expression; supplementary material Fig. S4], which represents another significant difference to the previously described mechanisms of vascular lumen formation.

Our data demonstrate that in zebrafish the CCVs form via a previously undescribed mode of lumen formation, which we term ‘lumen ensheathment’ (Fig. 5).

Analysis of the CCV microenvironment

Using electron microscopy and morpholino (MO)-based knockdown of gene function we analyzed the surrounding ultrastructures (Fig. 4M,N), the influence of blood flow (by *tnnt2a* MO; supplementary material Fig. S5B), possible co-migration with melanocytes (by *mitfa* MO; supplementary material Fig. S5D) and the role of the endoderm (by *sox32* MO; supplementary material Fig. S5F) in the migration of CCV cells. None of these was found to influence EC migration in the CCV.

Cdh5 is required for delamination as well as collective EC migration

Studies in mice and zebrafish have revealed the indispensable roles of Cdh5 and blood flow during vascular lumen formation (Strilić et al., 2009; Wang et al., 2010; Herwig et al., 2011). We investigated the role of these factors during delamination and lumenization in the CCV. At 32 hpf homozygous *cdh5*^{ubs8} mutant embryos showed no obvious morphological growth defects, but lacked circulation. Careful analysis revealed that in *cdh5*^{ubs8} mutant embryos the ECs

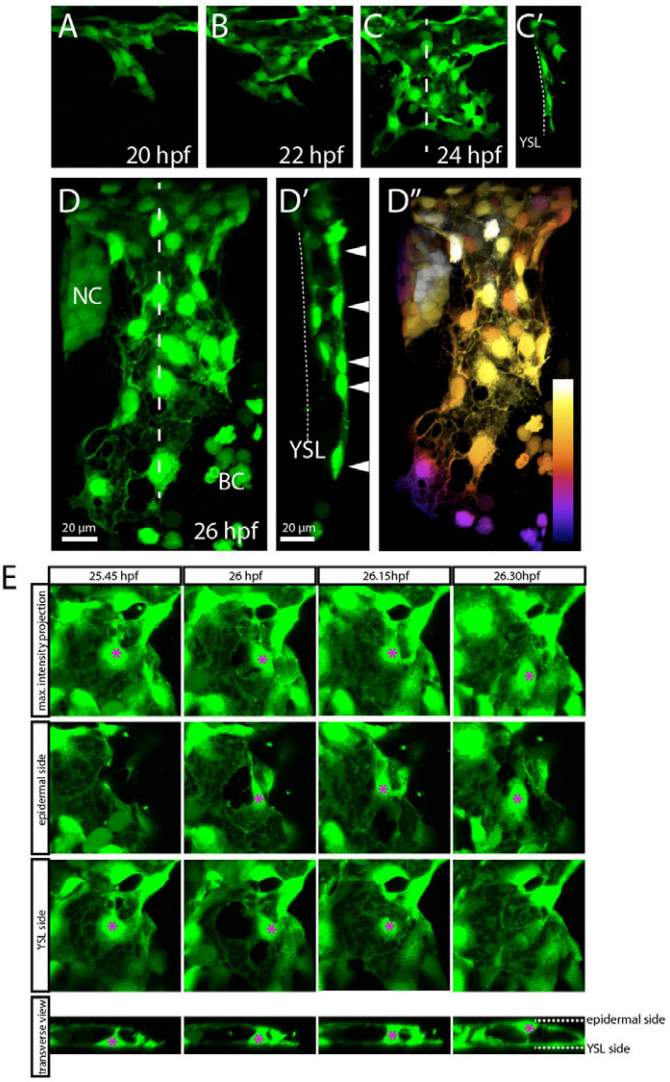

Fig. 3. ECs of the CCV delaminate from the migrating sheet and align around the lumen. Confocal projections from time-lapse movies of a *Tg(etsrp:EGFP)*^{ci1} (A-C′,E) or a *Tg(fli1a:EGFP)*^{y1} (D-D″) embryo, dorsolateral views. (**A-D″**) At 20 hpf, ECs start to migrate to form a monolayer on top of the YSL (A-C′). Individual ECs delaminate from the YSL side and thereby align around a lumen (D′,E). At 26 hpf, an initial lumenized open-ended cylinder is formed (D-D″). This cylinder becomes extended by the ECs underneath the epidermis (arrowheads in D′). Sagittal sections based on 3D reconstructions of C and D (at the levels indicated by the dashed lines) show a monolayer and no lumen (C′) and a lumen (D′). Arrowheads in D′ point to the ECs migrating to extend the CCV. (D″) Depth color coding of the confocal maximum projection shown in D. Proximal-most structures are white, whereas darker colors represent more distal structures. (**E**) Delamination of a single EC (asterisk) from the endothelial monolayer on top of the YSL to the epidermal side of the CCV. To visualize this process, the second and third panels contain only part of the maximum projection: in the panels labeled 'epidermal side', ECs located on the YSL side are cropped away, whereas in the panels labeled 'YSL side', ECs located on the epidermal side are cropped away. NC, neural crest; BC, blood cells; YSL, yolk syncytial layer.

forming the CCV failed to delaminate from the migrating monolayer to form a lumen (Fig. 6B′).

When we examined the length of the CCVs in *cdh5*^{ubs8} mutant embryos, we observed a reduction equivalent to the length of just one cell (Fig. 6B,E), indicating that at this developmental step EC migration is only minimally affected by Cdh5. Additionally, morphological cell adhesion was not impaired by lack of Cdh5 in the area of delamination (not shown). Our results indicate that Cdh5 is specifically required for the delamination that occurs during initial CCV formation.

To analyze the role of blood flow in lumen formation, we injected MOs targeting *cardiac troponin T2a* (*tnnt2a*) (Sehnert et al., 2002). Interestingly, the lack of blood flow does not influence the process of delamination or lumen formation in the CCV (Fig. 6D,D′).

Cadherin proteins have also been shown to be important during collective cell migration in epithelial sheets (Desai et al., 2009; Dupin et al., 2009). Therefore, we analyzed the expression of Cdh5 in the migrating CCV EC sheet. The ECs of the migrating sheet are connected by adherens and tight junctions (as shown by Cdh5 and ZO-1 staining; supplementary material Fig. S3).

Up to 55 hpf, the CCV has not connected to the endocardial cells of the heart inflow tract (data not shown) in *cdh5*^{ubs8} mutant embryos [but has in the wild type (WT); supplementary material Movie 3]. Therefore, we analyzed the behavior of single ECs in the migrating sheet of WT and *cdh5*^{ubs8} mutant embryos. Whereas in WT embryos the ECs in the collective sheet migrate in a highly directional manner towards the endocardium (Fig. 6F,H), this directionality is lost in *cdh5*^{ubs8} mutant embryos (Fig. 6G,H), where cells changed their direction during migration frequently, although their velocity was unaffected (Fig. 6H).

The number of ECs in the CCV is regulated by erythrocyte-derived Vegfc

To identify other molecular factors regulating CCV development, we analyzed the expression of various candidate genes. Of these, we detected domains of *vegfc* expression in the heart region and, with substantial variation between individual embryos, also along the CCV migration route (Fig. 7G, Fig. 8A). Vegfc signals via Flt4 (Vegfr3), which is strongly expressed in the developing veins (Fig. 7F). We therefore analyzed CCV development in embryos with altered Vegfc levels: either a *vegfc* mutant (*vegfc*^{hu6410}) or mRNA encoding a soluble version of human FLT4 (*sFLT4*) (Mäkinen et al., 2001) were used to lower Vegfc levels. *Vegfc* mRNA injection was employed to increase the level of Vegfc. Although loss of Vegfc did not influence EC migration (Fig. 7B), Vegfc appeared to regulate cell numbers in the developing CCVs. When Vegfc levels were elevated by *vegfc* mRNA injection, the CCVs were found to contain significantly more ECs than the CCVs of control embryos injected with *H2B-cherry* mRNA (Fig. 7C-E). Homozygous *vegfc*^{hu6410} mutant embryos displayed significantly reduced numbers of ECs compared with their WT or heterozygous mutant siblings (Fig. 7A,B,E; supplementary material Fig. S6A,B). In line with an increase in EC number in the CCVs of embryos injected with *vegfc* mRNA, we found more proliferating ECs (Fig. 7E; supplementary material Fig. S6D). By contrast, loss or reduction of Vegfc led to a reduced percentage of proliferating ECs (Fig. 7E; supplementary material Fig. S6E).

We observed patchy *vegfc* expression and a large variation in the expression domains between individual embryos (compare Fig. 7G with Fig. 8A). We hypothesized that this variation could result from *vegfc* expression by circulating blood cells. Blood cells are commonly found unevenly distributed in the circulatory system upon fixation, with the exception of the heart, where blood cells are usually 'trapped' within the heart chambers. In order to identify which cell population is the source of Vegfc, we injected MOs to ablate either macrophages (*pu.1* MO) (Rhodes et al., 2005) or

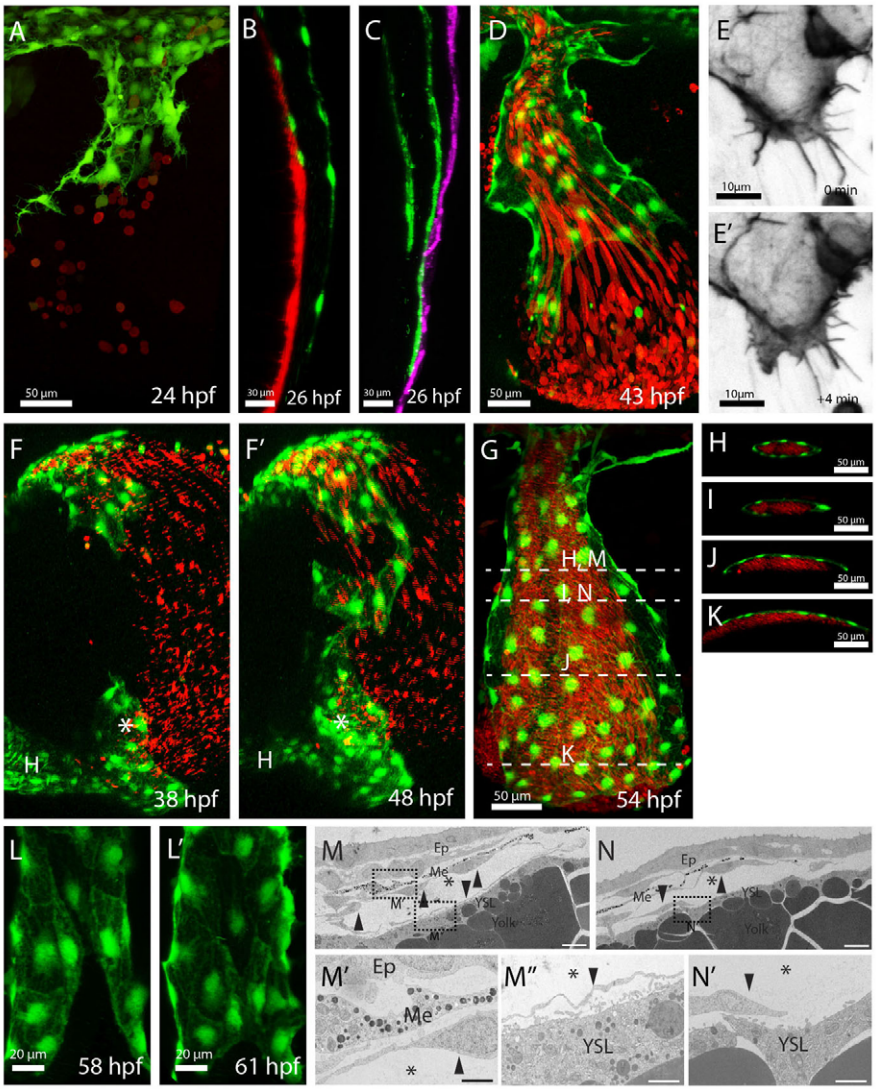

Fig. 4. ECs of the CCVs form an open-ended tube before the onset of blood flow and consecutively extend this open vessel. The ECs form an open-ended tube with blood exiting the EC-lined lumen (A,D); the lumen becomes extended by active EC migration (E,E′), during which ECs migrate as a sheet underneath the epidermis (C) and connect to ECs at the heart inflow tract (asterisk, F,F′). Consecutively, the ECs engulf the blood-filled lumen (I,N) and fuse on the YSL side (L,L′). (**A-L′**) Confocal projections of the developing CCVs, lateral views (A,D,E,G,L), sagittal views (B,C), lateral-ventral view (F) and transverse views (H-K). (D,E,F,L) Projections taken from confocal time-lapse movies. The developing vasculature was visualized by transgenic EGFP expression of *Tg(kdrl:EGFP)*^{s843} (B,D,F,G), *Tg(etsrp:EGFP)*^{ci1} (A,L), by transgenic mCherry expression of *Tg(kdrl:HsHRAS-mCherry)*^{s896} (green in C) or by vascular-specific lifeact-GFP expression [*Tg(UAS:lifeact-GFP)*^{mu271} *Tg(fli1ep:GAL4FF)*^{ubs4}] (E). The YSL was labeled by injection of mini-Ruby into the YSL (B). Erythrocytes are in red, visualized by transgenic dsRed expression of *Tg(gata1:dsRed)*^{sd2} (A,D,F-K). The epidermis is in purple [visualized by transgenic EGFP-caax expression of *Tg(krt4:EGFP-caax)*] (C). Note that the ECs underneath the epidermis extend the CCVs further (C) than on top of the YSL (B). ECs migrate actively with Actin-rich lamellipodia at their front (E,E′). (G-K) Ensheathment of the lumen by ECs; white bars in G indicate the approximate levels of the transverse views shown in H-K,M,N. (L,L′) Lumen closure on the YSL side. ECs of the epidermal side are cropped away. (**M-N′**) Electron micrograph (higher magnifications, M′,M″,N′) of the CCV of a 48 hpf embryo (scale bars: 10 μm). Arrowheads label ECs, asterisks the CCV lumen. Underneath the epidermis, ECs are next to melanocytes. On the other side of the lumen, ECs are located directly above the YSL. Note that in N there is no complete EC layer above the YSL. Ep, epidermis; Me, melanocytes; YSL, yolk syncytial layer.

erythrocytes (*gata1* MO) (Galloway et al., 2005). *In situ* hybridization showed that *vegfc* expression was unaffected in embryos injected with control MO or *pu.1* MO (arrow in Fig. 8B). However, ablation of erythrocytes by *gata1* MO injection resulted in loss of the *vegfc* expression domain in the heart region (arrow in Fig. 8C). In addition, we isolated erythrocytes at 24 hpf and 48 hpf from *Tg(gata1:dsRed)*^{sd2} transgenic embryos by FACS and performed RT-PCR analysis for *vegfc* on these isolated cell populations. This analysis confirmed that erythrocytes express *vegfc* at 48 hpf, whereas *vegfc* expression by the *gata1*$^{+}$ cell population was not, or barely, detectable at 24 hpf (Fig. 8J).

Consequently, we examined whether *vegfc* expression by erythrocytes constitutes the physiological source of Vegfc for regulating EC numbers in the CCVs. We again ablated either macrophages or erythrocytes by MO injection and counted EC numbers in the developing CCVs. We observed a significant reduction in the number of ECs in *gata1* MO-injected embryos (Fig. 8D), thereby identifying erythrocytes as a relevant source of

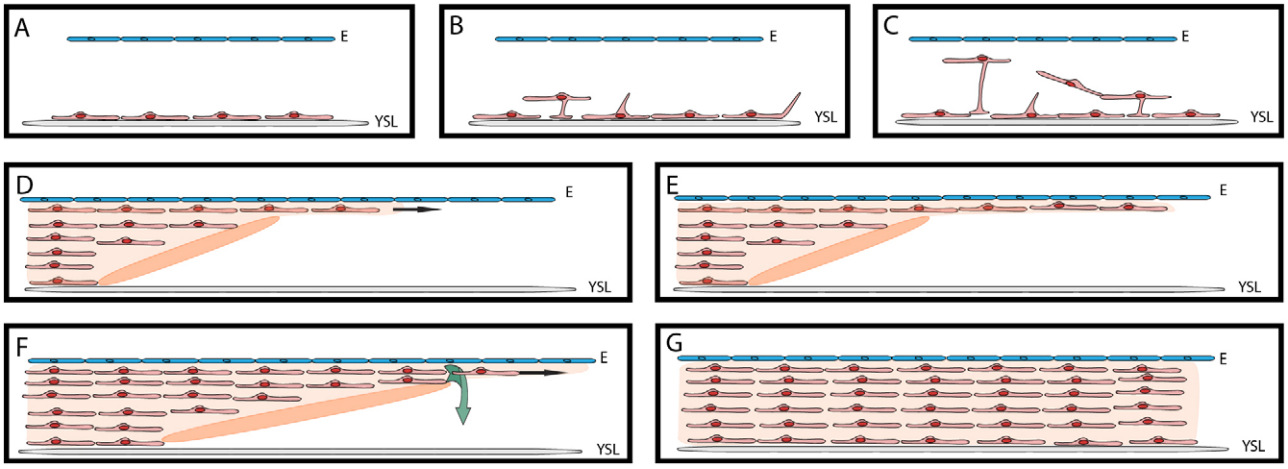

Fig. 5. Model of lumen formation by lumen ensheathment. Angioblasts individually migrate out and form a monolayer on top of the YSL (**A**, migration). Next, single angioblasts delaminate towards the epidermal side and align around the lumen (**B**,**C**, delamination), thereby forming an open-ended tube (**D**, alignment). The ECs on the epidermal side migrate faster and extend the lumen in the form of a sheet (**E**, extension). ECs at the edges of the sheet fold around and zip up the lumen (**F**, enclosure, zip up) by connecting on the YSL side, thereby forming a closed lumenized vessel (**G**). E, epidermis; YSL, yolk syncytial layer.

Vegfc for CCV development. In agreement with these results, we also showed that the lack of blood flow, and therefore the complete lack of erythrocytes in the CCVs, results in a significant decrease in EC number in the CCVs (Fig. 8E).

Since the CCV is the largest vessel in the zebrafish embryo at this developmental time point (Fig. 8F-H), it is reasonable to speculate that the ECs in the CCV are exposed to much higher levels of erythrocyte-derived Vegfc than in other developing vessels. In addition, we noted that the onset of proliferation in ECs of the CCV coincides with the onset of circulation and therefore with the exposure to blood (Fig. 8I). At 24 hpf, ECs in the CCV downregulate the angioblast marker *etsrp* (supplementary material Fig. S2F) and ECs in the CCV start to proliferate (as analyzed by BrdU incorporation, Fig. 8I). This timing supports our notion that erythrocyte-derived Vegfc regulates EC proliferation and thereby EC numbers in the growing CCVs.

DISCUSSION

We have analyzed the development of the CCV, starting from the earliest stages of angioblast specification up to the generation of a

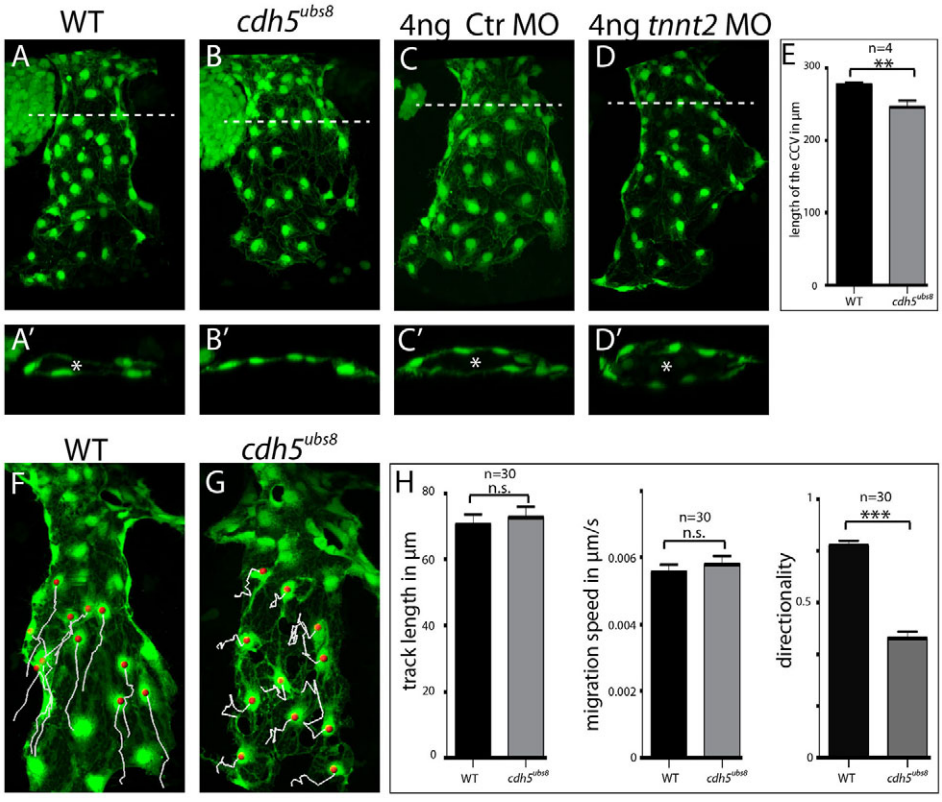

Fig. 6. Cdh5 is required for delamination and lumen extension in the CCV. (A-D,F,G) Confocal projections of the CCV at 32 hpf (A-D) and 36 hpf (F,G) of *Tg(kdrl:EGFP)*^{s843} (C,D,F,G) or *Tg(fli1a:EGFP)*^{y1} (A,B) embryos. (**A-D′**) ECs of *cdh5*^{ubs8} mutant embryos (B,B′) fail to delaminate and do not align around the lumen. Lack of blood flow (*tnnt2a* MO, D,D′) does not influence lumen formation. (A′-D′) Transverse sections of A-D, showing the lumen (asterisk) imaged at the level of the dashed line in A-D. (**E**) Quantification of the length of the CCV. (**F-H**) Directionality of collective migration is impaired in *cdh5*^{ubs8} mutant embryos (G, white lines), whereas migration track length or speed was unaffected (H). Single ECs (red dots) were tracked for 4 hours. $^{**}P<0.01$, $^{***}P<0.001$; n.s., not significant; error bars indicate s.e.m.

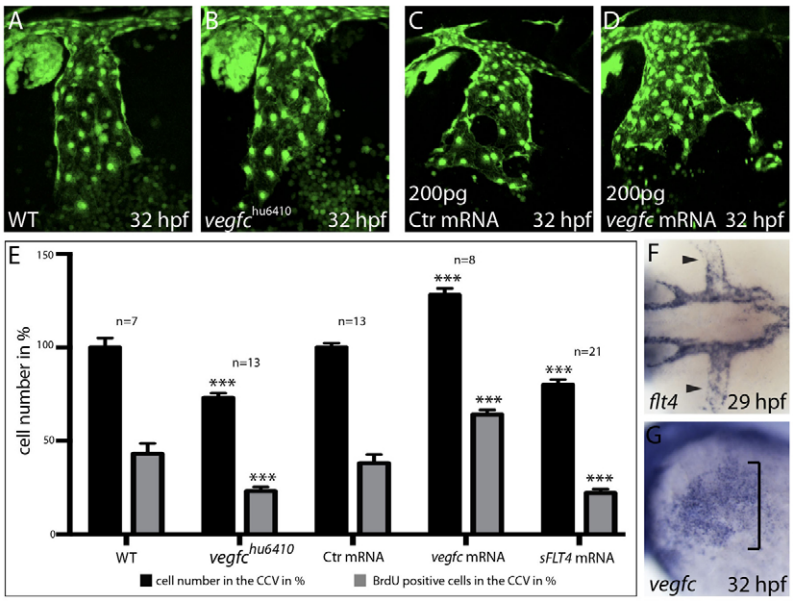

Fig. 7. Vegfc positively regulates EC proliferation in the CCVs. (**A-D**) Confocal projections of 32 hpf *Tg(fli1a:EGFP)*^{y1} wild-type (A) and homozygous *vegfc*^{hu6410} mutant *Tg(fli1a:EGFP)*^{y1} (B) embryos, and of *Tg(kdrl:EGFP)*^{s843} embryos injected with *H2B-cherry* mRNA (control, C) or *vegfc* mRNA (D). (**E**) Quantification of EC numbers and proliferation rates in the CCVs. EC proliferation is decreased in *vegfc*^{hu6410} or *sFLT4* mRNA-injected embryos (B,E) and increased upon *vegfc* overexpression (D,E). Embryos were pulsed with BrdU from 24-32 hpf. (**F**,**G**) Expression of *flt4* in the CCV (F, arrowheads) or *vegfc* in the area of CCV formation (G, bracket) detected by *in situ* hybridization at 29 hpf (F) or 32 hpf (G) in dorsal (F) or lateral (G) view. ***P<0.001; error bars indicate s.e.m. Ctr, control.

lumenized and functional vessel. We show that this particular component of the venous system develops by a completely novel mechanism, which we have termed lumen ensheathment.

Previous reports have suggested that angioblasts are prespecified within the LPM into venous and arterial precursors (Zhong et al., 2001). In our marker expression analysis we found no difference in the expression of *flt1* or *flt4* in angioblasts forming the bilateral cardinal veins, the CCVs or the LDA. Instead, we observed that *flt1* expression was downregulated during venous differentiation, whereas *flt4* [as shown previously (Thompson et al., 1998)] was downregulated in arteries. Similarly, arterial expression of such as *notch3*, *ephrin B2* (Lawson et al., 2001; Jin et al., 2005) or *dll4* (data not shown) is only observed once the ECs start differentiating at the final position of the DA.

However, we detected a difference in the timing of angioblast specification by analysis of *etsrp* expression as well as by time-lapse analysis and photoconversion experiments. We therefore propose that the temporal separation of the two populations forming the anterior arteries and veins could result in their spatial separation and constitute the underlying mechanism for the differential expression of arterial and venous marker genes.

Whereas other reports have focused on arterial and venous development in the tail of the zebrafish embryo (Torres-Vázquez et al., 2003; Jin et al., 2005; Herbert et al., 2009), we have focused on venous development and CCV formation in the anterior trunk. Although it was recently suggested that in the caudal tail venous ECs segregate from the ECs of the DA (Herbert et al., 2009), we found no common precursor structure for the arterial and venous ECs in the trunk.

Within the trunk region of the zebrafish embryo the arterial and venous morphology, with two bilateral DA and two bilateral cardinal veins, closely resembles the initial murine morphology (Swift and Weinstein, 2009). Therefore, the principles described here might also apply during mammalian development.

Different mechanisms of lumen formation have been discussed (Lubarsky and Krasnow, 2003) and recent reports have highlighted the differences in lumen formation with respect to the various vessels (Kamei et al., 2006; Blum et al., 2008; Iruela-Arispe and Davis, 2009; Strilić et al., 2009; Herwig et al., 2011). However, all previously described mechanisms rely on angiogenic vascular growth while maintaining an EC-lined, closed luminal space at all times. Surprisingly, we found that the CCV forms without respecting this requirement. Instead, it grows by directly assembling a tube from migrating ECs, not through a cord hollowing step but by Cdh5-dependent delamination of individual ECs and their subsequent alignment around the future lumen. Although the role of delamination has been extensively studied for many developmental processes, this is the first report to show that delamination plays an important role during vascular lumen formation.

By this process, the ECs initially create an open-ended tube, allowing for blood to exit the closed vascular network, re-entering it again at the sinus venosus. Consecutively, the CCV becomes extended by active migration of the ECs located underneath the epidermis towards the ECs of the heart inflow tract. Our results show that Cdh5 is uniquely required for the directionality of the collectively migrating ECs in the CCV. To enclose the lumen, ECs at the edges of the migrating sheet bend inwards, folding around the luminal space and therefore the blood stream. This morphogenetic process is very similar to the closure of the neural tube (Colas and Schoenwolf, 2001; Pyrgaki et al., 2010), suggesting a conserved role of this mechanism in lumen formation.

Many invertebrates have an open cardiovascular system, with hemolymph being pumped from the heart through blood vessels into the open hemocoel (Strilić et al., 2010). One might therefore speculate that the initially open CCV reflects an evolutionarily primitive stage of cardiovascular development. However, even in the human placenta maternal blood leaves the closed vessel system and enters the intervillous space. This indicates that within the cardiovascular system there are highly specialized vessels or areas, and that understanding the formation and the specializations of the individual vessels will reveal additional principles that might provide insight into the various misregulations that occur during disease.

We also demonstrate for the first time that circulating erythrocytes can regulate EC proliferation by the secretion of growth factors, namely Vegfc. Vegfc is mainly known for its role in lymphangiogenesis and regulation of lymphatic vessel size (Rissanen et al., 2003; Goldman et al., 2005), but few reports have addressed the role of Vegfc during blood vessel angiogenesis

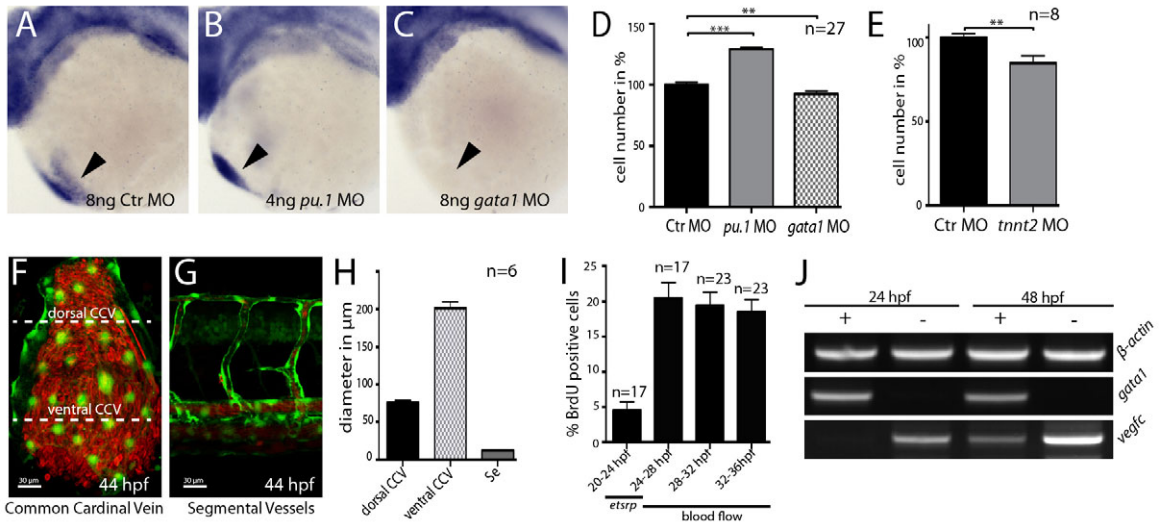

Fig. 8. Vegfc expressed from erythrocytes regulates EC numbers in the CCV. (**A-C**) Expression of *vegfc* in the region of the heart (arrows) in embryos injected with control MO (A), *pu.1* MO (B) or *gata1* MO (C) detected by *in situ* hybridization at 32 hpf; lateral views. (**D**,**E**) Quantification of EC numbers in the CCVs at 32 hpf (D) and 48 hpf (E). The number of ECs increased in embryos lacking macrophages (*pu.1* MO-injected, D) and decreased in embryos lacking erythrocytes (*gata1* MO-injected, D) or blood flow (*tnnt2a* MO-injected, E). (**F-H**) Confocal projections of *Tg(etsrp:EGFP)*^{ci1} CCV (F) and intersegmental vessel (Se) (G) at 44 hpf (lateral views) and comparison of the lumen diameter (H). The lumen diameter in the dorsal CCV is seven times larger and in the ventral CCV 20 times larger than that of the intersegmental vessel. Scale bars: 30 µm. (**I**) ECs start to proliferate with the onset of circulation. Until 24 hpf, ECs in the CCV still express the angioblast marker *etsrp* and only 5% proliferate. With the onset of circulation, proliferation of CCV ECs increases to 20%. Embryos were pulsed with BrdU at the indicated time points. (**J**) RT-PCR analysis of erythrocytes isolated from *Tg(gata1:DsRed)*^{sd2} embryos at 24 hpf and 48 hpf. *gata1:DsRed* positive (+) and negative (–) cells were isolated by FACS and analyzed for β-*actin*, *gata1* and *vegfc* expression. ***P*<0.01, ****P*<0.001; error bars indicate s.e.m.

(Covassin et al., 2006; Tammela et al., 2011). Of the hematopoietic cell lineages, previously only macrophages have been shown to aid vessel formation by Vegfc secretion (Tammela et al., 2011) or to regulate jugular lymph sac size (Gordon et al., 2010).

By contrast, we show for the first time that zebrafish erythrocytes can regulate EC proliferation. Zebrafish erythrocytes, like most vertebrate erythrocytes, contain transcriptionally active nuclei and are therefore able to produce and secrete growth factors. Similarly, mammalian erythrocytes, generated during primitive hematopoiesis, initially have nuclei. Although it has been proposed that they undergo enucleation in the circulation (Kingsley et al., 2004), this seems to occur long after they have entered circulation (McGrath et al., 2008). However, induction of vascular proliferation through growth factor secretion from erythrocytes might also play a role during early mammalian development. We show that deletion of the Pu.1 lineages, including all macrophages, leads to an increase in EC number of the CCVs (Fig. 8D), similar to the increase that results from *vegfc* overexpression. In zebrafish, deletion of the myeloid lineages leads to an increase in the erythroid lineage and vice versa (Galloway et al., 2005; Rhodes et al., 2005). We conclude that the higher EC number in the CCVs of embryos lacking macrophages is caused by an increase in erythrocytes and therefore higher levels of secreted Vegfc. Of note, there have been reports of other growth factors secreted into the blood stream, such as human BMP9, which was found in blood serum and shown to influence vascular quiescence (David et al., 2008).

In summary, our findings illustrate that angioblasts forming the CCVs initially share *flt1* and *flt4* expression with the angioblasts of the LDA, but differ in their time point of specification and consequently in the onset of migration. Additionally, we identify a novel mode of lumen formation, in which ECs of the future CCVs migrate, delaminate in a Cdh5-dependent manner and then align around an existing luminal space. Next, they migrate along the dorsal periphery of this lumen and thereby extend the CCV, at a time when circulating blood cells are already passing through. During this process, Cdh5 is important for the directionality of the collective EC migration. Subsequently, the CCV is completed by dorsal to ventral lumen enclosure. Although this process of CCV formation is flow independent, the proliferation of ECs within the CCV is regulated by erythrocytes that provide Vegfc.

Acknowledgements
We thank Aurelien Courtois and Jeroen Bussman for helpful discussion and suggestions; Ralf Adams and Friedemann Kiefer for critical comments on the manuscript; Stefania Nicoli for advice regarding the FACS sorting; Martin Stehling for FACS sorting; Reinhild Bußmann for fish husbandry; Karina Mildner for technical support for the electron microscopy analysis; Erez Raz for the lifeact-GFP plasmid; and Arndt Siekmann for providing the *gata1* MO.

Funding
C.S.M.H., A.S. and W.H. were funded by the North Rhine Westphalia (NRW) 'return fellowship'; T.K. was supported by a VENI grant from the Netherlands Organization for Scientific Research (NWO); S.S.-M. is supported by the KNAW; H.-G.B. and M.A. are supported by the Kantons Basel-Stadt and Basel-Land and by a grant from the Swiss National Science Foundation to M.A.

Competing interests statement
The authors declare no competing financial interests.

Author contributions
C.S.M.H. and W.H. designed the study, interpreted the data and wrote the paper. C.S.M.H., A.S. and D.Z. performed the experiments and analyzed the data. T.K., H.-G.B., M.A. and S.S.-M. contributed zebrafish mutants and reagents, and edited the manuscript.

Supplementary material
Supplementary material available online at
http://dev.biologists.org/lookup/suppl/doi:10.1242/dev.091876/-/DC1

References

Ando, R., Hama, H., Yamamoto-Hino, M., Mizuno, H. and Miyawaki, A. (2002). An optical marker based on the UV-induced green-to-red photoconversion of a fluorescent protein. *Proc. Natl. Acad. Sci. USA* **99**, 12651-12656.

Asakawa, K., Suster, M. L., Mizusawa, K., Nagayoshi, S., Kotani, T., Urasaki, A., Kishimoto, Y., Hibi, M. and Kawakami, K. (2008). Genetic dissection of neural circuits by Tol2 transposon-mediated Gal4 gene and enhancer trapping in zebrafish. *Proc. Natl. Acad. Sci. USA* **105**, 1255-1260.

Atkins, G. B., Jain, M. K. and Hamik, A. (2011). Endothelial differentiation: molecular mechanisms of specification and heterogeneity. *Arterioscler. Thromb. Vasc. Biol.* **31**, 1476-1484.

Baer, M. M., Chanut-Delalande, H. and Affolter, M. (2009). Cellular and molecular mechanisms underlying the formation of biological tubes. *Curr. Top. Dev. Biol.* **89**, 137-162.

Blum, Y., Belting, H. G., Ellertsdottir, E., Herwig, L., Lüders, F. and Affolter, M. (2008). Complex cell rearrangements during intersegmental vessel sprouting and vessel fusion in the zebrafish embryo. *Dev. Biol.* **316**, 312-322.

Bussmann, J., Bakkers, J. and Schulte-Merker, S. (2007). Early endocardial morphogenesis requires Scl/Tal1. *PLoS Genet.* **3**, e140.

Carmeliet, P. (2000). Mechanisms of angiogenesis and arteriogenesis. *Nat. Med.* **6**, 389-395.

Chi, N. C., Shaw, R. M., De Val, S., Kang, G., Jan, L. Y., Black, B. L. and Stainier, D. Y. (2008). Foxn4 directly regulates tbx2b expression and atrioventricular canal formation. *Genes Dev.* **22**, 734-739.

Chung, W. S. and Stainier, D. Y. (2008). Intra-endodermal interactions are required for pancreatic beta cell induction. *Dev. Cell* **14**, 582-593.

Colas, J. F. and Schoenwolf, G. C. (2001). Towards a cellular and molecular understanding of neurulation. *Dev. Dyn.* **221**, 117-145.

Covassin, L. D., Villefranc, J. A., Kacergis, M. C., Weinstein, B. M. and Lawson, N. D. (2006). Distinct genetic interactions between multiple Vegf receptors are required for development of different blood vessel types in zebrafish. *Proc. Natl. Acad. Sci. USA* **103**, 6554-6559.

David, L., Mallet, C., Keramidas, M., Lamandé, N., Gasc, J. M., Dupuis-Girod, S., Plauchu, H., Feige, J. J. and Bailly, S. (2008). Bone morphogenetic protein-9 is a circulating vascular quiescence factor. *Circ. Res.* **102**, 914-922.

Desai, R. A., Gao, L., Raghavan, S., Liu, W. F. and Chen, C. S. (2009). Cell polarity triggered by cell-cell adhesion via E-cadherin. *J. Cell Sci.* **122**, 905-911.

Dupin, I., Camand, E. and Etienne-Manneville, S. (2009). Classical cadherins control nucleus and centrosome position and cell polarity. *J. Cell Biol.* **185**, 779-786.

Dyer, L. A. and Patterson, C. (2010). Development of the endothelium: an emphasis on heterogeneity. *Semin. Thromb. Hemost.* **36**, 227-235.

Ellertsdóttir, E., Lenard, A., Blum, Y., Krudewig, A., Herwig, L., Affolter, M. and Belting, H. G. (2010). Vascular morphogenesis in the zebrafish embryo. *Dev. Biol.* **341**, 56-65.

Galloway, J. L., Wingert, R. A., Thisse, C., Thisse, B. and Zon, L. I. (2005). Loss of gata1 but not gata2 converts erythropoiesis to myelopoiesis in zebrafish embryos. *Dev. Cell* **8**, 109-116.

Goldman, J., Le, T. X., Skobe, M. and Swartz, M. A. (2005). Overexpression of VEGF-C causes transient lymphatic hyperplasia but not increased lymphangiogenesis in regenerating skin. *Circ. Res.* **96**, 1193-1199.

Gordon, E. J., Rao, S., Pollard, J. W., Nutt, S. L., Lang, R. A. and Harvey, N. L. (2010). Macrophages define dermal lymphatic vessel calibre during development by regulating lymphatic endothelial cell proliferation. *Development* **137**, 3899-3910.

Hatta, K., Tsujii, H. and Omura, T. (2006). Cell tracking using a photoconvertible fluorescent protein. *Nat. Protoc.* **1**, 960-967.

Herbert, S. P., Huisken, J., Kim, T. N., Feldman, M. E., Houseman, B. T., Wang, R. A., Shokat, K. M. and Stainier, D. Y. (2009). Arterial-venous segregation by selective cell sprouting: an alternative mode of blood vessel formation. *Science* **326**, 294-298.

Herwig, L., Blum, Y., Krudewig, A., Ellertsdottir, E., Lenard, A., Belting, H. G. and Affolter, M. (2011). Distinct cellular mechanisms of blood vessel fusion in the zebrafish embryo. *Curr. Biol.* **21**, 1942-1948.

Herzog, W., Müller, K., Huisken, J. and Stainier, D. Y. (2009). Genetic evidence for a noncanonical function of seryl-tRNA synthetase in vascular development. *Circ. Res.* **104**, 1260-1266.

Hogan, B. M., Bos, F. L., Bussmann, J., Witte, M., Chi, N. C., Duckers, H. J. and Schulte-Merker, S. (2009a). Ccbe1 is required for embryonic lymphangiogenesis and venous sprouting. *Nat. Genet.* **41**, 396-398.

Hogan, B. M., Herpers, R., Witte, M., Heloterä, H., Alitalo, K., Duckers, H. J. and Schulte-Merker, S. (2009b). Vegfc/Flt4 signalling is suppressed by Dll4 in developing zebrafish intersegmental arteries. *Development* **136**, 4001-4009.

Iruela-Arispe, M. L. and Davis, G. E. (2009). Cellular and molecular mechanisms of vascular lumen formation. *Dev. Cell* **16**, 222-231.

Isogai, S., Horiguchi, M. and Weinstein, B. M. (2001). The vascular anatomy of the developing zebrafish: an atlas of embryonic and early larval development. *Dev. Biol.* **230**, 278-301.

Jin, S. W., Beis, D., Mitchell, T., Chen, J. N. and Stainier, D. Y. (2005). Cellular and molecular analyses of vascular tube and lumen formation in zebrafish. *Development* **132**, 5199-5209.

Joukov, V., Pajusola, K., Kaipainen, A., Chilov, D., Lahtinen, I., Kukk, E., Saksela, O., Kalkkinen, N. and Alitalo, K. (1996). A novel vascular endothelial growth factor, VEGF-C, is a ligand for the Flt4 (VEGFR-3) and KDR (VEGFR-2) receptor tyrosine kinases. *EMBO J.* **15**, 1751.

Kamei, M., Saunders, W. B., Bayless, K. J., Dye, L., Davis, G. E. and Weinstein, B. M. (2006). Endothelial tubes assemble from intracellular vacuoles in vivo. *Nature* **442**, 453-456.

Karkkainen, M. J., Haiko, P., Sainio, K., Partanen, J., Taipale, J., Petrova, T. V., Jeltsch, M., Jackson, D. G., Talikka, M., Rauvala, H. et al. (2004). Vascular endothelial growth factor C is required for sprouting of the first lymphatic vessels from embryonic veins. *Nat. Immunol.* **5**, 74-80.

Kimmel, C. B., Ballard, W. W., Kimmel, S. R., Ullmann, B. and Schilling, T. F. (1995). Stages of embryonic development of the zebrafish. *Dev. Dyn.* **203**, 253-310.

Kingsley, P. D., Malik, J., Fantauzzo, K. A. and Palis, J. (2004). Yolk sac-derived primitive erythroblasts enucleate during mammalian embryogenesis. *Blood* **104**, 19-25.

Krens, S. F., Mollmert, S. and Heisenberg, C. P. (2011). Enveloping cell-layer differentiation at the surface of zebrafish germ-layer tissue explants. *Proc. Natl. Acad. Sci. USA* **108**, E9-E10.

Küchler, A. M., Gjini, E., Peterson-Maduro, J., Cancilla, B., Wolburg, H. and Schulte-Merker, S. (2006). Development of the zebrafish lymphatic system requires VEGFC signaling. *Curr. Biol.* **16**, 1244-1248.

Larson, J. D., Wadman, S. A., Chen, E., Kerley, L., Clark, K. J., Eide, M., Lippert, S., Nasevicius, A., Ekker, S. C., Hackett, P. B. et al. (2004). Expression of VE-cadherin in zebrafish embryos: a new tool to evaluate vascular development. *Dev. Dyn.* **231**, 204-213.

Lawson, N. D. and Weinstein, B. M. (2002a). In vivo imaging of embryonic vascular development using transgenic zebrafish. *Dev. Biol.* **248**, 307-318.

Lawson, N. D. and Weinstein, B. M. (2002b). Arteries and veins: making a difference with zebrafish. *Nat. Rev. Genet.* **3**, 674-682.

Lawson, N. D., Scheer, N., Pham, V. N., Kim, C. H., Chitnis, A. B., Campos-Ortega, J. A. and Weinstein, B. M. (2001). Notch signaling is required for arterial-venous differentiation during embryonic vascular development. *Development* **128**, 3675-3683.

Lee, J., Gray, A., Yuan, J., Luoh, S. M., Avraham, H. and Wood, W. I. (1996). Vascular endothelial growth factor-related protein: a ligand and specific activator of the tyrosine kinase receptor Flt4. *Proc. Natl. Acad. Sci. USA* **93**, 1988-1992.

Lubarsky, B. and Krasnow, M. A. (2003). Tube morphogenesis: making and shaping biological tubes. *Cell* **112**, 19-28.

Mäkinen, T., Jussila, L., Veikkola, T., Karpanen, T., Kettunen, M. I., Pulkkanen, K. J., Kauppinen, R., Jackson, D. G., Kubo, H., Nishikawa, S. et al. (2001). Inhibition of lymphangiogenesis with resulting lymphedema in transgenic mice expressing soluble VEGF receptor-3. *Nat. Med.* **7**, 199-205.

McGrath, K. E., Kingsley, P. D., Koniski, A. D., Porter, R. L., Bushnell, T. P. and Palis, J. (2008). Enucleation of primitive erythroid cells generates a transient population of 'pyrenocytes' in the mammalian fetus. *Blood* **111**, 2409-2417.

Megason, S. G. (2009). In toto imaging of embryogenesis with confocal time-lapse microscopy. *Methods Mol. Biol.* **546**, 317-332.

Nasevicius, A. and Ekker, S. C. (2000). Effective targeted gene 'knockdown' in zebrafish. *Nat. Genet.* **26**, 216-220.

Proulx, K., Lu, A. and Sumanas, S. (2010). Cranial vasculature in zebrafish forms by angioblast cluster-derived angiogenesis. *Dev. Biol.* **348**, 34-46.

Pyrgaki, C., Trainor, P., Hadjantonakis, A. K. and Niswander, L. (2010). Dynamic imaging of mammalian neural tube closure. *Dev. Biol.* **344**, 941-947.

Rhodes, J., Hagen, A., Hsu, K., Deng, M., Liu, T. X., Look, A. T. and Kanki, J. P. (2005). Interplay of pu.1 and gata1 determines myelo-erythroid progenitor cell fate in zebrafish. *Dev. Cell* **8**, 97-108.

Riedl, J., Crevenna, A. H., Kessenbrock, K., Yu, J. H., Neukirchen, D., Bista, M., Bradke, F., Jenne, D., Holak, T. A., Werb, Z. et al. (2008). Lifeact: a versatile marker to visualize F-actin. *Nat. Methods* **5**, 605-607.

Rissanen, T. T., Markkanen, J. E., Gruchala, M., Heikura, T., Puranen, A., Kettunen, M. I., Kholová, I., Kauppinen, R. A., Achen, M. G., Stacker, S. A. et al. (2003). VEGF-D is the strongest angiogenic and lymphangiogenic effector among VEGFs delivered into skeletal muscle via adenoviruses. *Circ. Res.* **92**, 1098-1106.

Robu, M. E., Larson, J. D., Nasevicius, A., Beiraghi, S., Brenner, C., Farber, S. A. and Ekker, S. C. (2007). p53 activation by knockdown technologies. *PLoS Genet.* **3**, e78.

Sakaguchi, T., Kuroiwa, A. and Takeda, H. (2001). A novel sox gene, 226D7, acts downstream of Nodal signaling to specify endoderm precursors in zebrafish. *Mech. Dev.* **107**, 25-38.

Santoro, M. M., Samuel, T., Mitchell, T., Reed, J. C. and Stainier, D. Y. (2007). Birc2 (clap1) regulates endothelial cell integrity and blood vessel homeostasis. *Nat. Genet.* **39**, 1397-1402.

Schieber, N. L., Nixon, S. J., Webb, R. I., Oorschot, V. M. and Parton, R. G. (2010). Modern approaches for ultrastructural analysis of the zebrafish embryo. *Methods Cell Biol.* **96**, 425-442.
Schoenebeck, J. J., Keegan, B. R. and Yelon, D. (2007). Vessel and blood specification override cardiac potential in anterior mesoderm. *Dev. Cell* **13**, 254-267.
Schulte-Merker, S. (2002). Looking at embryos. In *Zebrafish: A Practical Approach* (ed. C. Nüsslein-Vollhard and R. Dahm), pp. 39-58. New York, NY: Oxford University Press.
Sehnert, A. J., Huq, A., Weinstein, B. M., Walker, C., Fishman, M. and Stainier, D. Y. (2002). Cardiac troponin T is essential in sarcomere assembly and cardiac contractility. *Nat. Genet.* **31**, 106-110.
Strilić, B., Kucera, T., Eglinger, J., Hughes, M. R., McNagny, K. M., Tsukita, S., Dejana, E., Ferrara, N. and Lammert, E. (2009). The molecular basis of vascular lumen formation in the developing mouse aorta. *Dev. Cell* **17**, 505-515.
Strilić, B., Kucera, T. and Lammert, E. (2010). Formation of cardiovascular tubes in invertebrates and vertebrates. *Cell. Mol. Life Sci.* **67**, 3209-3218.
Swift, M. R. and Weinstein, B. M. (2009). Arterial-venous specification during development. *Circ. Res.* **104**, 576-588.
Tammela, T., Zarkada, G., Nurmi, H., Jakobsson, L., Heinolainen, K., Tvorogov, D., Zheng, W., Franco, C. A., Murtomäki, A., Aranda, E. et al. (2011). VEGFR-3 controls tip to stalk conversion at vessel fusion sites by reinforcing Notch signalling. *Nat. Cell Biol.* **13**, 1202-1213.
Thisse, C. and Thisse, B. (2008). High-resolution in situ hybridization to whole-mount zebrafish embryos. *Nat. Protoc.* **3**, 59-69.
Thompson, M. A., Ransom, D. G., Pratt, S. J., MacLennan, H., Kieran, M. W., Detrich, H. W., 3rd, Vail, B., Huber, T. L., Paw, B., Brownlie, A. J. et al. (1998). The cloche and spadetail genes differentially affect hematopoiesis and vasculogenesis. *Dev. Biol.* **197**, 248-269.
Torres-Vázquez, J., Kamei, M. and Weinstein, B. M. (2003). Molecular distinction between arteries and veins. *Cell Tissue Res.* **314**, 43-59.
Traver, D., Paw, B. H., Poss, K. D., Penberthy, W. T., Lin, S. and Zon, L. I. (2003). Transplantation and in vivo imaging of multilineage engraftment in zebrafish bloodless mutants. *Nat. Immunol.* **4**, 1238-1246.
Veikkola, T. and Alitalo, K. (1999). VEGFs, receptors and angiogenesis. *Semin. Cancer Biol.* **9**, 211-220.
Wang, Y., Kaiser, M. S., Larson, J. D., Nasevicius, A., Clark, K. J., Wadman, S. A., Roberg-Perez, S. E., Ekker, S. C., Hackett, P. B., McGrail, M. et al. (2010). Moesin1 and Ve-cadherin are required in endothelial cells during in vivo tubulogenesis. *Development* **137**, 3119-3128.
Westerfield, M. (1993). *The Zebrafish Book.* Eugene, OR: University of Oregon Press.
Wiley, D. M., Kim, J. D., Hao, J., Hong, C. C., Bautch, V. L. and Jin, S. W. (2011). Distinct signalling pathways regulate sprouting angiogenesis from the dorsal aorta and the axial vein. *Nat. Cell Biol.* **13**, 686-692.
Yaniv, K., Isogai, S., Castranova, D., Dye, L., Hitomi, J. and Weinstein, B. M. (2006). Live imaging of lymphatic development in the zebrafish. *Nat. Med.* **12**, 711-716.
Zhong, T. P., Childs, S., Leu, J. P. and Fishman, M. C. (2001). Gridlock signalling pathway fashions the first embryonic artery. *Nature* **414**, 216-220.

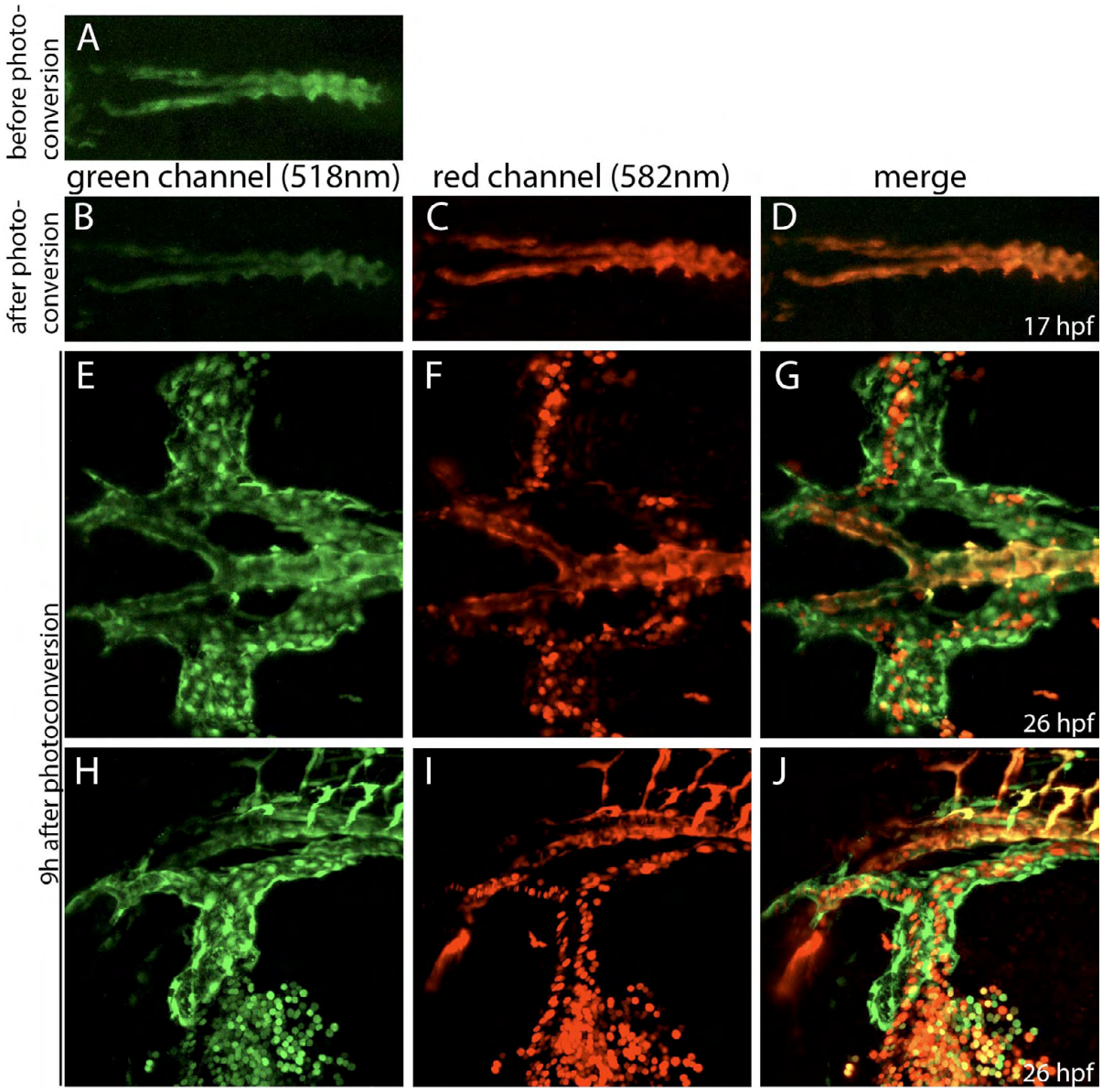

Fig. S1. The angioblasts forming the bilateral cardinal veins and the common cardinal veins (CCVs) are specified as a second population and at a separate time point to the population forming the lateral dorsal aortae. (A-J) Confocal projections of *Tg(fli1ep:GAL4FF)*^{ubs4} *(UAS:KAEDE)*^{rk8} embryos at the indicated time points. Endothelial cells (ECs) (and blood cells) were visualized by transgenic Kaede expression. (A-G) Dorsal views; (H-J) lateral views. (**A**) EC-specific Kaede expression before photoconversion at 17 hpf, before the second population of angioblasts starts to express Kaede. (**B**) EC-specific non-converted Kaede (green) expression after photoconversion, indicating that not all Kaede protein was converted. (**C**) EC-specific converted Kaede (red) expression after photoconversion. (**D**) Merged image of converted and non-converted Kaede expression after photoconversion. (**E**) Non-converted Kaede expression, reflecting newly synthesized Kaede protein, imaged 9 hours after photoconversion. Green Kaede protein can be detected in the LDA and the bilateral cardinal veins as well as in the CCVs. (**F**) Nine hours after photoconversion, converted Kaede (red) expression can only be detected in the LDA, but not in the veins. (**G**) Merged image of the red and green channel showing Kaede expression 9 hours after photoconversion. Note that the transgenic Kaede expression can also be detected in blood cells. (**H**) Non-converted Kaede expression 9 hours after photoconversion is detected in the LDA and the bilateral cardinal veins as well as in the CCV. (**I**) Converted Kaede expression 9 hours after photoconversion is only detected in the LDA. (**J**) Merged image of the red and green channel showing Kaede expression 9 hours after photoconversion. Note that the transgenic Kaede expression can also be detected in blood cells.

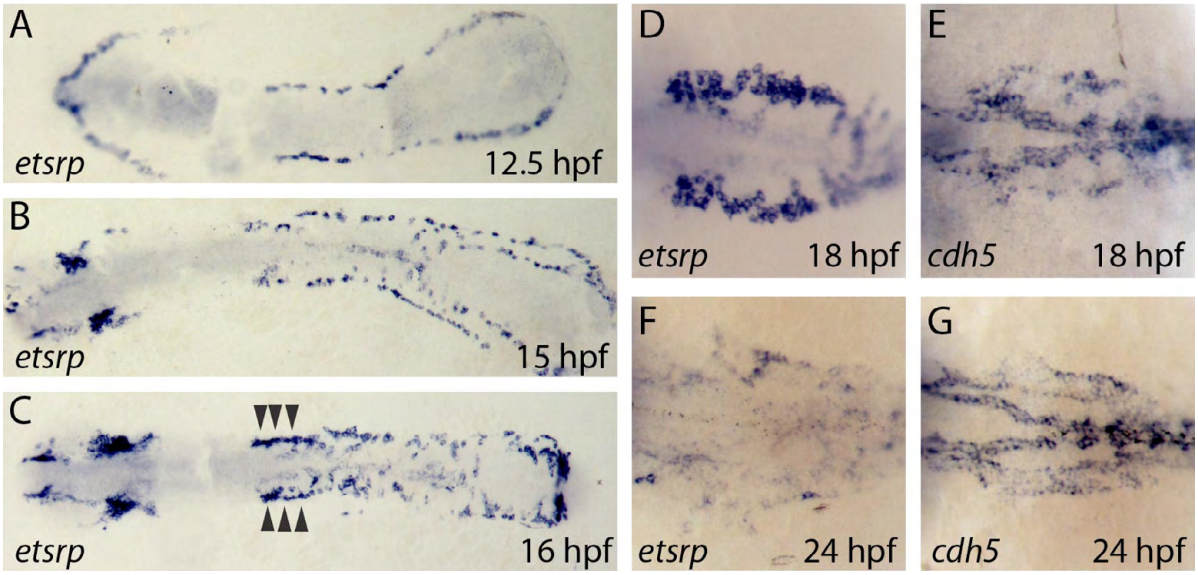

Fig. S2. *etsrp* is strongly expressed in newly specified angioblasts but becomes downregulated after angioblast migration. (A-D,F) Brightfield images showing expression of *etsrp* (etv2) detected by *in situ* hybridization in embryos at the indicated time points (dorsal views). (A-C) Flat-mounted embryos; (D-G) higher magnification of the trunk region. (E,G) Brightfield images showing expression of *cadherin 5* (*cdh5*) detected by *in situ* hybridization in embryos at the indicated time points (dorsal views). (**A**) *etsrp* mRNA can be detected in angioblasts within the lateral plate mesoderm. (**B**) *etsrp* mRNA levels are lower in angioblasts that have already migrated to the midline. (**C**) High *etsrp* expression in angioblasts that will form the bilateral cardinal veins/CCVs (arrowheads). (**D**) Cells forming the bilateral cardinal veins/CCVs show high levels of *etsrp* expression, whereas *etsrp* expression is very weak in the ECs of the LDA. (**F**) *etsrp* expression in the bilateral cardinal veins/CCVs decreases over time until it is no longer detectable. (**E**,**G**) *cdh5* expression labels all angioblasts. CCV, common cardinal vein; LDA, lateral dorsal aortae.

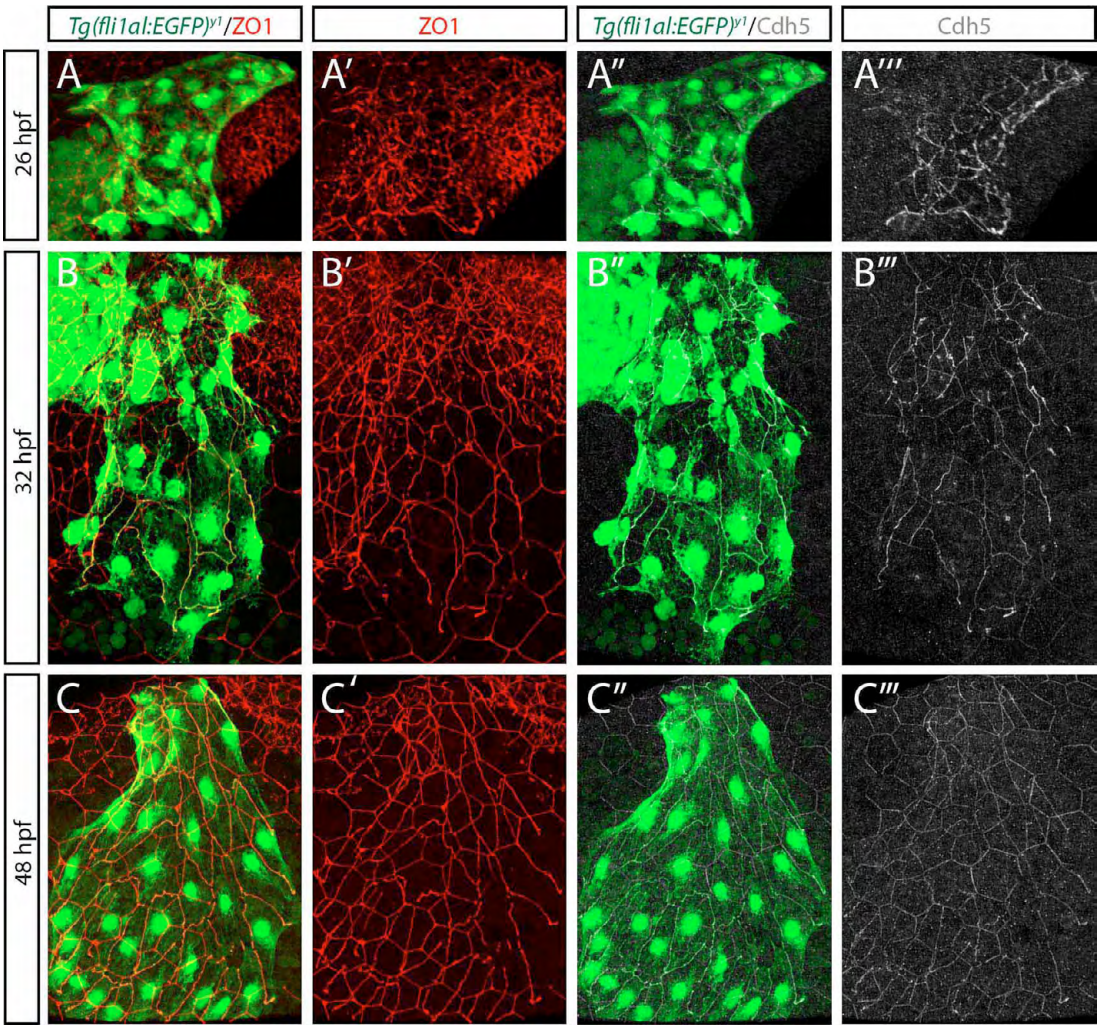

Fig. S3. ECs of the CCV form tight and adherens junctions. (A-C) Fluorescent confocal images of immunostainings of the junctional proteins ZO-1 and Cdh5 at the indicated time points; lateral views. The developing vasculature is visualized by transgenic EGFP expression of *Tg(fli1a:EGFP)^{y1}*. (**A-A‴**) ECs of the CCV express the tight junction protein ZO-1 and the adherens junction protein Cdh5 at 26 hpf. (**B-B‴**) ECs of the CCV express the tight junction protein ZO-1 and the adherens junction protein Cdh5 at 32 hpf. (**C-C‴**) ECs of the CCV express the tight junction protein ZO-1 and the adherens junction protein Cdh5 at 48 hpf. Note that the epidermis shows nonspecific Cdh5 staining at 48 hpf.

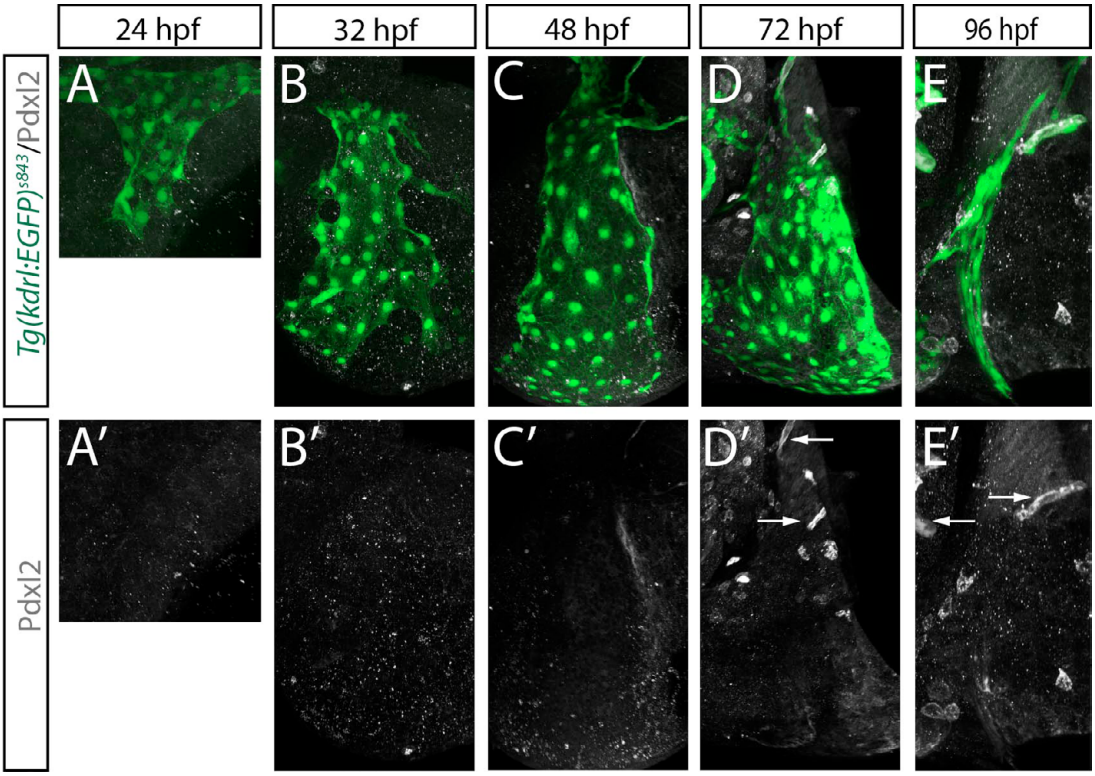

Fig. S4. ECs of the CCV have no apical polarization (analyzed by Podocalyxin-like 2 expression). (**A-E′**) Fluorescent confocal images of immunostainings of Podocalyxin 2 (Pdxl2) at the indicated time points; lateral views. The developing vasculature is visualized by transgenic EGFP expression of *Tg(kdrl:EGFP)*^{s843}. ECs of the CCV do not form Pdxl2-positive membrane compartments, whereas ECs in the fin bud (arrows in D′ and right arrow in E′) and ECs in the aortic arches (left arrow in E′) form apical membrane compartments as indicated by Pdxl2 staining.

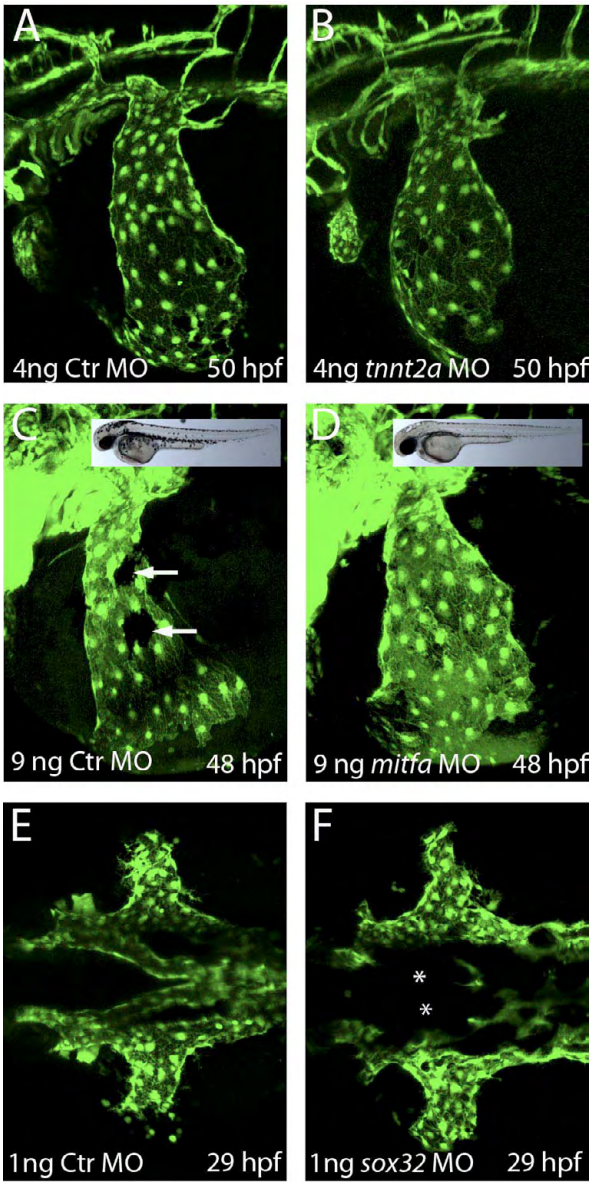

Fig. S5. CCV development is not affected by blood flow, melanocytes or endoderm. (A-F) Confocal fluorescent images of transgenic zebrafish embryos at the indicated time points. ECs were visualized by transgenic EGFP expression [*Tg(kdrl:EGFP)*^{s843}]. (A-D) Lateral views; (E,F) dorsal views. (**A**,**B**) Embryos injected with control MO (A) or with *tnnt2a* MO (B). Note that the CCV developed normally in the absence of blood flow in *tnnt2a* MO-injected embryos (B). (**C**,**D**) Embryos injected with control MO (C) or *mitfa* MO (D). Note that although *mitfa* MO-injected embryos had no melanocytes (compare brightfield images, insets in C and D) the CCVs developed normally. Arrows indicate melanocytes in C. (**E**,**F**) Embryos injected with control MO (E) or with *sox32* MO (F). Note that in the absence of endoderm the LDA fail to form (asterisks), whereas the CCVs develop (F). CCV, common cardinal vein; Ctr, control; LDA, lateral dorsal aortae; WT, wild type.

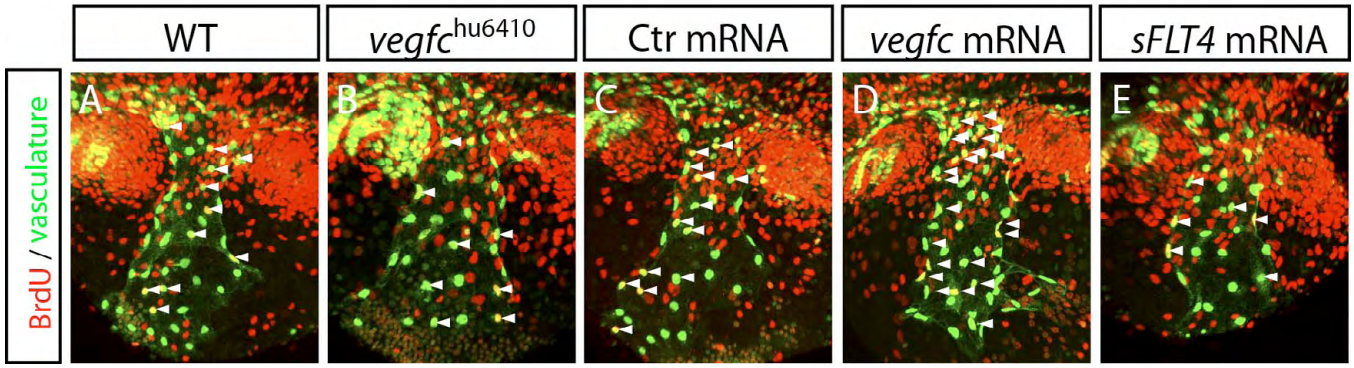

Fig. S6. Vegfc positively regulates EC proliferation in the CCVs. Confocal projections of 32 hpf *Tg(kdrl:EGFP)*^{s843} wild-type siblings (**A**), homozygous *vegfc*^{hu6410} mutant embryos (**B**) or embryos injected with *H2B-cherry* mRNA (control, **C**), *vegfc* mRNA (**D**) or *sFLT4* mRNA (**E**), all pulsed with BrdU from 24-32 hpf. BrdU staining is shown in red; vascular ECs are visualized in green by staining for GFP expression [of *Tg(fli1al:EGFP)*^{y1} in A,B and of *Tg(kdrl:EGFP)*^{s843} in C-E]. EC proliferation is decreased in *vegfc*^{hu6410} (B) or *sFLT4* mRNA-injected (E) embryos and increased upon *vegfc* overexpression (D). Arrowheads mark BrdU-positive ECs in the CCV.

Movie 1. Angioblasts forming the bilateral cardinal veins and the CCVs become specified at a different time point than the cells forming the arteries. Confocal time-lapse movie of the trunk of a transgenic zebrafish embryo imaged in dorsal view. The vasculature was visualized by transgenic EGFP expression [*Tg(fli1al:EGFP)*^{y1}]. This movie shows that an initially specified population of angioblasts forms the lateral dorsal aortae, whereas a second, later-specified population of angioblasts will form the bilateral cardinal veins and the CCVs. Starting at 14 hpf, the time-lapse series covers a period of 8 hours with one confocal *z*-stack recorded every 15 minutes.

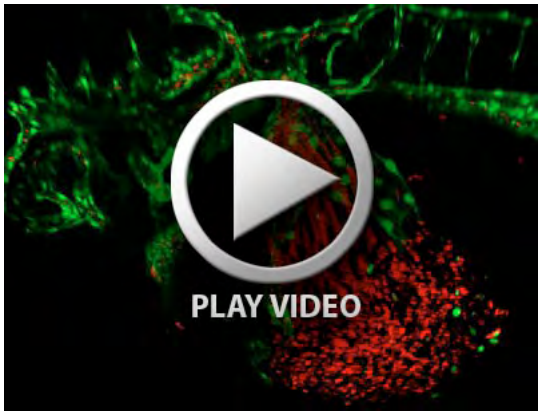

Movie 2. ECs in the CCV migrate around the flowing blood to form the CCV. Confocal time-lapse movie of a double-transgenic embryo. The developing vasculature is shown in green [visualized by transgenic EGFP expression of *Tg(kdrl:EGFP)*^{s843}] and the blood is shown in red [visualized by transgenic dsRed expression of *Tg(gata1:dsRed)*^{sd2}]; lateral views. Starting at 33 hpf, this time-lapse series covers a period of 20 hours with one confocal *z*-stack recorded every 15 minutes. Note that blood flows out of the open-ended CCV, while the ECs migrate towards the endocardial cells at the sinus venosus of the heart.

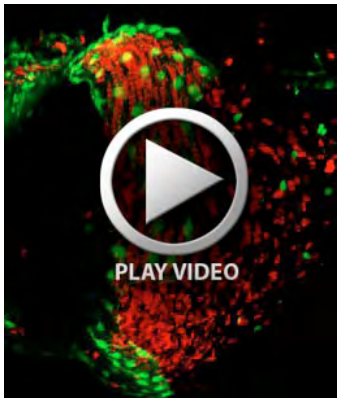

Movie 3. ECs in the CCV connect to the endocard. Confocal time-lapse movie of a double-transgenic embryo. The developing vasculature is shown in green [visualized by transgenic EGFP expression of *Tg(kdrl:EGFP)*^{s843}] and the blood is shown in red [visualized by transgenic dsRed expression of *Tg(gata1:dsRed)*^{sd2}]; lateral views. Starting at 33 hpf this time-lapse series covers a period of 20 hours with one confocal *z*-stack recorded every 15 minutes. Note that that the endocardial cells do not migrate, while the ECs of the CCV migrate towards the endocardial cells at the sinus venosus of the heart.

Movie 4. ECs of the CCV actively migrate. Confocal time-lapse movie of a double-transgenic embryo. The actin cytoskeleton of the ECs is labeled by transgenic GFP expression in *Tg(UAS:lifeact-GFP)*^{mu271} *Tg(fli1ep:GAL4FF)*^{ubs4} double-transgenic embryos; lateral views. Starting at 41 hpf this time-lapse series covers a period of 5 hours with one confocal *z*-stack recorded every 2 minutes. Note that ECs migrate with Actin-rich lamellipodia in the front.

Movie 5. ECs of the CCV fuse distally to close the lumen of the CCV. Confocal time-lapse movie of a double-transgenic embryo. The developing vasculature is shown in green [visualized by transgenic EGFP expression of *Tg(etsrp:EGFP)*^{ci1}]; lateral views. Starting at 58 hpf this time-lapse series covers a period of 12 hours with one confocal *z*-stack recorded every 7 minutes. After ECs ensheath the blood stream, they close the lumen at the YSL side from dorsal to ventral. ECs at the epidermal side are cropped away.